A hierarchical Bayesian space-time model for radioactivity deposition

Swarup De* and Alvaro E. Faria
The Open University, UK

June 11, 2009

Abstract

A hierarchical Bayesian space-time (HBST) model, an extension of the class of dynamic linear models to space-time processes, is proposed for the statistical modelling of radioactivity deposition after a nuclear accident. It explicitly handles uncertainties associated with (i) predictions of depositions from a long-range atmospheric dispersal model, (ii) in-situ gamma ray measurements and (iii) spatial interpolations. Unlike existing environmental statistical models, the HBST model also accounts for an established food chain contamination model called ECOSYS for which it provides data assimilation capabilities. Three distinct formulations of the HBST model were applied to assimilate real data of radioactivity deposition from the Chernobyl accident in southern Germany. Two of those formulations differ on the functional form of their spatial covariance matrices while the third, a normal inverse-Wishart model, allows the spatial covariances to "learn" from data within the usual Bayesian paradigm. The later is shown to outperform the former models both in short and medium term forecasting as well as in a predictive interpolation test that took some measurements as out-of-sample.

Key words: Atmospheric dispersal model; Dynamic linear model; Hierarchical model; Isotropy; Markov random field process; Spatial modelling

Address for correspondence: Swarup De, Department of Mathematics and Statistics, The Open University, Walton Hall, Milton Keynes, MK7 6AA, United Kingdom.
E-mail: s.de@open.ac.uk

1 Introduction

In this paper we propose and test a statistical model for uncertainty handling and data assimilation associated with the ground deposition of radioactivity after a nuclear accident. The model makes use of all information available during the accident in order to provide the best possible estimation of the levels of ground contamination by the released radioisotopes (together with a measure of their quality) for decision support purposes at various levels in nuclear emergencies, such as distribution of iodine tablets, sheltering advice and evacuation. For this, a hierarchical Bayesian spatio-temporal (HBST) model was developed to coherently combine information coming from established physical and environmental models with in-situ near ground radioactivity measurements.

The scenario we considered here is one of a severe accident in a nuclear plant with radioactive releases into the environment. This can typically be characterized as having four distinct phases:

(1) a pre-release phase, when the in-plant conditions deteriorate in such a way that the accidental release of radioactive material (source term) is about to occur;

(2) a release phase, when while being released the source term is dispersed into the atmosphere;

(3) an early post-release phase, when while being dispersed, the released masses of radionuclides are also partially deposited in time at diverse locations, contaminating soil, plants, waters, and thus, entering the human food chain; and

(4) a late post-release phase where contamination passes through animal and food chains and impacts on long term environmental factors.

The pre-release and release phases (1) and (2) above are associated with the early stages of the accident, that is, with a time scale ranging from few minutes to one or two days of duration. The post-release phases (3) and (4) are associated with the medium and long term and time scales ranging from days to years.

Diverse deterministic but typically very complex physical and environmental models have been developed to describe a nuclear accident with its related contamination and effects during each phase. Examples of those for the early phase are the in-plant status probabilistic belief net for source term estimation (Smedley *et al.*, 1996) and the Lagrangian K-model model for long-range atmospheric dispersal (Lauritzen *et al.*, 2006). For the later stages, the ECOSYS (Müller and Pröhl, 1993) describes the food chain

contamination. Because of their hazardous environmental and health effects, any auxiliary experiments that have been performed are either limited in their association with the real scenario (for example, tracer experiments which use non-toxic smoke emissions typically in constant wind field environment) or are the product of strict control (like lab tests on plants exposure to radiation). The result of this is that current physical and environmental models are largely descriptive.

Data from the rare accidents that have occurred are not generally available for two reasons, the sensitivity of such information and the lack of proper measurement protocols during the emission (it is only in the last few years that these protocols have been implemented across Europe for example). When available they are useful for the modelling related to the geographic region they come from but not for other regions.

Typically, such models have great complexity, lack of linearity and an internal integrity. They can be thought as machines which take a function of outputs from previous modules (except for the first), vectors of observations and vectors of known covariates as their inputs to produce outputs. The outputs of this module can then be used as one of the components of the inputs of a subsequent module.

Part of the work we describe here has been developed in the RODOS (Real time Online Decision Support) system, an EU project for decision support in nuclear emergencies, that includes a module for each of the above phases. Note that all opinions expressed as well as the statistical methodology developed in this paper are of the authors.

Similarly to Gamerman *et al.* (2006), we adopt a state-space approach based on an extension of the dynamic linear model of West and Harrison (1997) to our spatio-temporal process. However, unlike Gamerman *et al.* (2006), our approach includes specific environmental and physical models in its formulation. In fact, the development of our integrated hierarchical Bayesian approach is oriented to include the ECOSYS model of Müller and Pröhl (1993) as a particular case. The ECOSYS is a detailed physical-biological model developed to explain the spread of radioactive contamination within the food chain with possible consequences on the human exposure doses. It includes modules for ground deposition, food chain contamination and human exposure. The ground deposition module, the one we will be focusing on in this paper, assesses the radiological consequences of short-term depositions of radionuclides in diverse types of soil and plants. Our proposed HBST model handles in a rather natural and structured way the uncertainties associated with the ECOSYS model as we shall see. In addition, this model allows fairly easily not only the combination of information coming from different sources (such as estimations based on atmospheric dispersal and near-ground radioactivity measurements) but also the inclusion of new components, when needed (such as trends and seasonality for example),

by augmentation of vectors and matrices only. Also, at any time the probability density of all variables will be dynamically updated by the information available up to that time. That is, the joint density is updated as new data become available with no need for the full data set to be collected before updating can take place. Moreover, different types of measured data need not all be available at every monitoring station as usually will be the case. In practice, different stations will have different measuring resources, for example, stations equipped to measure γ-dose rates not necessarily will be prepared to measure air concentration and/or amount of rainfall. To handle nuclide specific wet and dry deposited activities on soil, the HBST model was formulated with three main components. Those components are represented by variables and parameters associated with total deposited activity and proportions of both specific radioisotopes and wet deposition relative to the total ground deposition mass at each site of interest.

Because we allow learning (from data) on the covariance structure related to the model, part of our results here are comparable to those of Le and Zidek (1992). Basically, it consists of the application of standard multivariate normal-wishart conjugate analysis (Anderson, 1984). However, differently from Le and Zidek, in our case significant temporal structures are included (temporal autocorrelation is allowed) as well as an explicit direct modelling of spatial interpolations. The latter allows for smoothness constraints on the covariance estimates through the specification of a suitable spatial interpolation matrix.

The HBST model focuses on the interface between components of the atmospheric dispersal, K-model, and the food chain, ECOSYS. We shall make use of outputs from the K-model, such as its predictions of radioactivity deposition for a regular spatial grid, as inputs to the HBST model. Those predictions are treated as data and combined with in-situ deposition measurements taken at sites which are usually off-grid locations. In practice, the deposition measurements (or other measurements from which ground deposition can be calculated, such as near-ground air concentrations together with rainfall intensities and near-ground gamma dose rates) will not be available for all sites of interest. In fact, there will be a number of fixed monitoring stations irregularly and sparsely separated over the region of interest. Some mobile measuring capability should be possible however in small scale. Also, there is a subtle interface question between the atmospheric dispersal K-model and the ECOSYS which is that of what deposition is meant in each model. Because, deposition for ECOSYS is not only nuclide but also plant specific, we assume (for the models' reconciliation sake) that near-ground deposition at a certain site corresponds to deposition on soil.

The proposed HBST model was applied to real data of the 1986 Chernobyl's accident contamination of Bavaria in southern Germany. In fact, three versions of the HBST

model combined predictions at fixed regular grid points from the long range atmospheric K-model mentioned above with measured (off-grid) near-ground contamination in Bavaria to produce estimations (actual and predictive) of the contamination profile.

The accident at the Chernobyl nuclear reactor (in northern Ukraine, near the border with Belarus) that occurred on 26 April 1986 was the most serious accident ever to occur in the nuclear power industry. The accident happened during an experimental test of the electrical control system when the reactor was being shut down for routine maintenance. A sudden power surge caused a chain of events leading to the destruction of the reactor's core, the severe damaging of the plant's building and ultimately to the release of considerable amounts of radioactive materials to the atmosphere. The leaking core was exposed to the elements for ten days before engineers were able to seal the building. The radioactive gases and particles released in the accident were initially carried by the wind in westerly and northerly directions. On subsequent days, distinct wind directions prevailed. The deposition of radionuclides was primarily governed by any precipitation occurring during the passage of the radioactive cloud, leading to a complex and variable exposure pattern throughout the affected region and as well as to other European countries including Germany as we shall see.

The paper is structured as follows. In Section 2, the HBST model which allows for uncertainty handling and data assimilation of ECOSYS is introduced. The deposition module of ECOSYS is briefly introduced in Subsection 2.1. Subsection 2.2 introduces notation associated with the HBST model as well as a graphical model that establishes a link between the statistical and the ECOSYS models. Subsection 2.3 describes the HBST model formulation. Subsections 2.4 and 2.5 defines the three different formulations of the HBST model to the deposition data. In Section 3, an application of HBST model is described. Subsection 3.1, real data of Chernobyl's near-ground radioactive deposition in a region in southern Germany is described. Subsection 3.2, described the long range atmospheric dispersal K-model. Section 4 describes the main results of the application of the three HBST models. This Section starts by describing the values of the input parameters of the HBST models in Subsection 4.1. The predictive performances of the HBST models are described in Subsections 4.2. Section 5 concludes the paper. Appendix A and Appendix B show the prior-to-posterior updating equations for the HBST models with known and unknown observational covariance matrix respectively.

2 The HBST model

In this section we describe the proposed HBST model in detail. We start by briefly describing the deposition module of ECOSYS as well as the link between the ECOSYS and the HBST model. We have made use of graphical representations for those in order to facilitate those descriptions. The graphical representations also allow to depict the important conditional independence structure associated with the models. After that, a general version of a Gaussian HBST model is defined. To comply with the Gaussian errors assumption, the defined variables and parameters were transformed. In practice, the contamination variables will not be strictly Gaussian since, for example, we cannot have negative values of contamination. Also, proportion variables which values belong to the interval (0,1) are obviously non-Gaussian. This problem is solved by the use of appropriate transformations which allows the treatment of errors as Gaussian as we shall see.

2.1 The deposition module of ECOSYS

As mentioned in the introduction, we shall focus on the deposition module of ECOSYS which models multiple-nuclide radioactivity depositions to soil and plants.

In the deposition stage (3) of the accident (described in the Introduction), ECOSYS calculates for a general site $\mathbf{s}$ with cartesian coordinates $(x, y) \in \mathbb{R}^2$, the total radioactivity $A(i, j, \mathbf{s})$ produced by the deposited isotope type j which is intercepted by the plant type i. The type j radionuclide deposition to soil at site $\mathbf{s}$ is treated separately for its effects on root uptakes and resuspension to air. They are otherwise obtained similarly to the plants.

The calculations for every time t, omitted here for simplicity, are performed by decomposing the total deposition of radioactivity, A, into wet and dry components. The dry component caused by dry deposition counts for the air activity concentration contribution to the contamination while the wet component counts for both air concentration and rainfall contributions. Thus, if $A_{dry}(i, j, \mathbf{s})$ is the component of the total contamination caused by dry depositions of isotope j on plant i at the location $\mathbf{s}$, and $A_{wet}(i, j, \mathbf{s})$ is the wet deposition component of isotope j at $\mathbf{s}$, then

$$A(i, j, \mathbf{s}) = A_{dry}(i, j, \mathbf{s}) + A_{wet}(i, j, \mathbf{s}) \ ,$$

where $A_{wet}(i, j, \mathbf{s}) = f_w(i, j, \mathbf{s})A_{wet}(j, \mathbf{s})$ with $f_w(i, j, \mathbf{s})$ called the *interception fraction* of isotope j for plants type i at site $\mathbf{s}$, determined from specific retention coefficients and

rainfall amounts. The dry contamination component $A_{dry}(i, j, \mathbf{s})$ is obtained from the time-integrated activity concentration of isotope j in air at $\mathbf{s}$, $\bar{C}_{air}(j, \mathbf{s})$, as $A_{dry}(i, j, \mathbf{s}) = v_g(i, j)\bar{C}_{air}(j, \mathbf{s})$, where $v_g(i, j)$ is the *deposition velocity* of isotope j on the plants type i at $\mathbf{s}$, determined with the use of leaf area indexes. Please refer to Müller and Pröhl (1993) and Bleher and Jacob (1993) for further details.

2.2 The HBST model's spatial components

Our model defines a regular grid with n points over the geographic region of interest. Each grid point represents a location for which the long range atmospheric dispersal model will generate a prediction. The network of m fixed monitoring stations will be usually located off-grid.

In practice, a monitoring station will be able to measure at least one of the following data:

(i) instantaneous air concentrations (c_{air}) and γ-dose rates (γ-Dose) which are informative about the time (and nuclide) aggregated total depositions,

(ii) γ-spectrometry (γ-Spec), informative about the proportions of different radionuclides on the total depositions, and

(iii) rainfall intensity (r), giving information about the proportion of wet deposition relative to the total.

Omitting the time and space indexes (t and $\mathbf{s}$ respectively) for simplicity, the HBST model has three main components Z, P and Q associated with the above described data:

Z: total ground radioactivity deposition,

P_j: proportion of the radionuclide j ($j = 1, \ldots, k$) in the total ground deposition, and

Q: fraction of wet deposited radioactivity from the total ground deposition.

Those components allow not only the assimilation of the above mentioned measurements but also the uncertainty calculations relative to the nuclide specific wet and dry radioactivity intakes for different types of plants as we shall see.

With the above components introduced, we can draw the *directed acyclic graph* (DAG) of Figure 1 which makes a link between our statistical HBST model and a pragmatic version of the deposition module of the food chain ECOSYS model. The main difference between the theoretical ECOSYS described in the previous section and its pragmatic

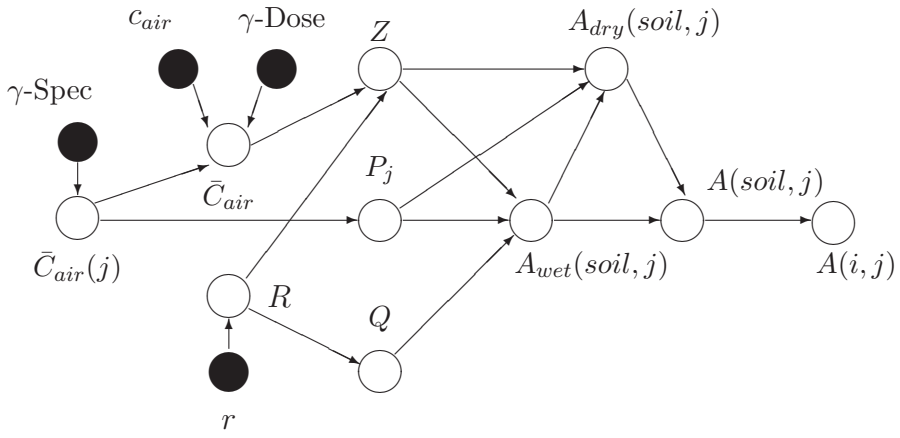

Figure 1: A directed acyclic graph linking the HBST and the ECOSYS models

version shown in the DAG below is that the activities in plants $A(i, j, \mathbf{s})$ are obtained from the activities in soil $A(soil, j, \mathbf{s})$. This is due to fact that we are making use of near-ground measurements of activities as surrogate for measures of deposition in soil. Plant specific activities can be estimated from those with the use of appropriate factors as described by Müller and Pröhl (1993).

The graph depicts the logical associations between the variables of the statistical model including the sources of informative data. The filled circle nodes represent sources of information (data) such as gamma dose rates readings (γ-Dose), gamma ray spectrometry (γ-Spec), instantaneous air concentrations (c_{air}) and rainfall intensities (r).

Measurements of time-integrated air concentrations, $\bar{C}_{air}(j, \mathbf{s})$, are usually obtained by integrating instantaneous air concentration readings, $C_{air}(j, \mathbf{s}, t)$ in time. They can also be obtained from γ-dose rate readings as described in Bleher and Jacob (1993). However, the isotopic composition in air concentrations needs γ-spectrometry readings to be determined. Readings of γ-ray spectrum in their turn can also give information on measures of instantaneous air concentrations. In fact, γ-dose rates readings give information on total aggregated time-integrated air concentrations $\bar{C}_{air}(\mathbf{s}) = \sum_j \bar{C}_{air}(j, \mathbf{s})$, while γ-spectrum readings give information on $\bar{C}_{air}(j, \mathbf{s})$, that is on the components of $\bar{C}_{air}(\mathbf{s})$.

Note that in this graph, the HBST model components Z, $P(j)$ and Q separate the ECOSYS inputs $\bar{C}_{air}$ and R from the activity outputs $A_{dry}(soil, j)$ and $A_{wet}(soil, j)$ (as well as $A(soil, j)$ and $A(i, j)$) such that once those components are known the output variables will have no further (new) information to be gained from the input variables. In fact, the following conditional independencies can be stated from the DAG of Figure 1:

(a) $Z \amalg P_j \amalg Q | \bar{C}_{air}, R$ (but $Z \not\amalg P_j \not\amalg Q$ unconditionally);

(b) $A(i,j), A(soil,j) \amalg Z, P_j, Q | A_{wet}(soil,j), A_{dry}(soil,j)$;

(c) $\bar{C}_{air}, R \amalg A_{dry}(soil,j), A_{wet}(soil,j) | Z, P_j, Q$

Those conditional independence statements are used to simplify the joint probability distribution functions of those variables which can be factorized accordingly. Please refer to Smith (1989) for examples of how to read conditional independence statements from directed acyclic graphs as well as to factorise joint probability distribution functions according to such statements.

The nuclide specific activity intake by plant i at a location $\mathbf{s}$, $A(i,j,\mathbf{s})$, can be obtained from $A(soil,j,\mathbf{s})$, since $A_{wet}(j,\mathbf{s}) = A_{wet}(soil,j,\mathbf{s}) = Z_{\mathbf{s}} P_{j,\mathbf{s}} Q_{\mathbf{s}}$ and $A_{dry}(soil,j,\mathbf{s}) = Z_{\mathbf{s}} P_{j,\mathbf{s}}[1-Q_{\mathbf{s}}]$. In fact, the nuclide specific wet deposited activity at a location $\mathbf{s}$ is assumed to be deposition over soil, that is $A_{wet}(soil,j,\mathbf{s})$ for nuclide j. From that, the wet deposition at $\mathbf{s}$ for grassland is calculated as $A_{wet}(grass,j,\mathbf{s}) = f_w(grass,j,\mathbf{s}) A_{wet}(soil,j,\mathbf{s})$, where $f_w(grass,j,\mathbf{s})$ is the interception fraction of nuclide j for grass at site $\mathbf{s}$. The wet deposition of nuclide j for all other types of plants is calculated in a similar way from $A_{wet}(grass,j,\mathbf{s})$ as $A_{wet}(i,j,\mathbf{s}) = \left[\frac{f_w(i,j,\mathbf{s})}{f_w(grass,j,\mathbf{s})}\right] A_{wet}(grass,j,\mathbf{s})$ for each plant i.

Before we start defining the HBST model in more detail, we would like to point out that all the variables associated with the components Z, P_j and Q above as well as their related parameters have been transformed. Those transformations were necessary so that the model could comply with the assumption of Gaussian errors. In particular, we have used logarithmic transformations for the variables associated with total ground deposition as well as neutral to the right (NTTR) transformations of Walker and Muliere (1997) for the variables associated with the proportions components. The NTTR transformations guarantee that the proportion variables add up to unity and can be assumed to be Gaussian.

2.3 The HBST model formulation

The random variables we define below are associated with the components Z, P_j and Q described above. Because vectors of those variables will need to be decomposed into subcomponents grouped according to their origin, we shall use throughout the text the subscripts D and M, to indicate the spatial location of data represented, that is, D will represent grid points and M monitoring station points. We use prime to denote transposition throughout the paper.

Let, at a time t ($t = 1, \ldots, \tau$), $\mathbf{Z}_{Dt} = (Z_{D1t}, \ldots, Z_{Dnt})'$where Z_{Dit} is the observed total radioactivity deposition at grid point i ($i = 1, \ldots, n$) at time t, and $\mathbf{Z}_{Mt} = (Z_{M1t}, \ldots, Z_{Mmt})'$ where Z_{Mit} is the observed total radioactivity deposition at monitoring station site i ($i = 1, \ldots, m$) at time t.

Similarly, let $\mathbf{P}_{Dt} = (\mathbf{P}_{D1t}, \ldots, \mathbf{P}_{Dnt})$ with $\mathbf{P}_{Dit} = (P_{Di1t}, \ldots, P_{Dikt})'$ where P_{Dijt} is the proportion (from the total deposition Z_{Dit}) of radionuclide j deposited at the grid point i at time t, and $\mathbf{P}_{Mt} = (\mathbf{P}_{M1t}, \ldots, \mathbf{P}_{Mmt})$ with $\mathbf{P}_{Mit} = (P_{Mi1t}, \ldots, P_{Mikt})'$ where P_{Mijt} is the proportion (from the total deposition Z_{Mit}) of radionuclide j deposited at the off-grid measuring site i at time t.

Also, let $\mathbf{Q}_{Dt} = (Q_{D1t}, \ldots, Q_{Dnt})'$ where Q_{Dit} is the proportion (from the total deposition Z_{Dit}) of wet deposited radioactivity at the grid point i at time t, and $\mathbf{Q}_{Mt} = (Q_{M1t}, \ldots, Q_{Mmt})'$ where Q_{Mit} is the proportion (from the total deposition Z_{Mit}) of wet deposited radioactivity at the grid point i at time t.

Now, let $\mathbf{Y}_{Dt} = (\mathbf{Z}_{Dt}, \mathbf{P}_{Dt}, \mathbf{Q}_{Dt})'$ and $\mathbf{Y}_{Mt} = (\mathbf{Z}_{Mt}, \mathbf{P}_{Mt}, \mathbf{Q}_{Mt})'$. Let $\mathbf{\Theta}_{Dt} = (\theta_{Dt}, \pi_{Dt}, \rho_{Dt})'$, $\mathbf{\Theta}_{Mt} = (\theta_{Mt}, \pi_{Mt}, \rho_{Mt})'$ be the state vectors associated with the observational vectors $\mathbf{Y}_{Dt}$ and $\mathbf{Y}_{Mt}$ respectively, where the components θ_{Dt} and θ_{Mt} are vectors with elements θ_{it} ($i = 1, \ldots, n$ for grid points or $i = 1, \ldots, m$ for monitoring station sites) interpreted as the real *unknown* total radioactivity deposition at location i at time t. Similarly, each element π_{ijt} of π_{it} is the real *unknown* proportion of isotope j in the total deposition θ_{it} at location i at time t; and each element ρ_{it} of ρ_{ct} ($c = D$ or M) is the real *unknown* proportion of wet deposited activity from the total deposition at location i at time t. We can now define the HBST model by the following observation, interpolation and time evolution equations.

The *observation equation* is

$$\begin{bmatrix} \mathbf{Y}_{Dt} \\ \mathbf{Y}_{Mt} \end{bmatrix} = \begin{bmatrix} \mathbf{\Theta}_{Dt} \\ \mathbf{\Theta}_{Mt} \end{bmatrix} + \begin{bmatrix} \nu_{Dt} \\ \nu_{Mt} \end{bmatrix}, \quad \begin{bmatrix} \nu_{Dt} \\ \nu_{Mt} \end{bmatrix} \sim N(\mathbf{0}, V_t) \tag{1}$$

where the observational error terms associated with grid points, $\nu_{Dt} = (\nu_{Z_{Dt}}, \nu_{P_{Dt}}, \nu_{Q_{Dt}})'$, and monitoring stations, $\nu_{Mt} = (\nu_{Z_{Mt}}, \nu_{P_{Mt}}, \nu_{Q_{Mt}})'$, are assumed independent and normally distributed with zero mean vector and covariance matrix $V_t = diag(V_{Dt}, V_{Mt})$ with $V_{Dt} = diag(V_{Z_{Dt}}, V_{P_{Dt}}, V_{Q_{Dt}})$ and $V_{Mt} = diag(V_{Z_{Mt}}, V_{P_{Mt}}, V_{Q_{Mt}})$. For each component c ($c = D, M$), $V_{Z_{ct}}$ is a covariance matrix with each element $v_{Z_{ct}}(i, j) = cov(\nu_{Z_{cit}}, \nu_{Z_{cjt}})$ being the covariance between the total deposition error at site i, $\nu_{Z_{cit}}$, and the total deposition error at site j, $\nu_{Z_{cjt}}$, at time t. The dimension of $V_{Z_{ct}}$ is $(n \times n)$ when $c = D$ and $(m \times m)$ when $c = M$. $V_{P_{ct}}$ is a covariance matrix with each element $v_{P_{ct}}(i, j, s, l) = cov(\nu_{P_{cist}}, \nu_{P_{cjlt}})$ being the covariance between the observational error of proportion of nuclide i at site s,

$\nu_{P_{cist}}$, and $\nu_{P_{cjlt}}$, at time t. The dimension of $V_{P_{ct}}$ is $(nk \times nk)$ and $(mk \times mk)$ for $c = D$ and $c = M$ respectively. $V_{Q_{ct}}$ is a covariance matrix with each element $v_{Q_{cijt}} = cov(\nu_{Q_{cit}}, \nu_{Q_{cjt}})$ being the covariance between the error of proportion of wet deposition at site i, $\nu_{Q_{cit}}$, and $\nu_{Q_{cjt}}$ at time t. The dimension of $V_{Q_{ct}}$ is $(n \times n)$ and $(m \times m)$ for $c = D$ and $c = M$ respectively.

The *interpolation equation* is

$$\mathbf{\Theta}_{Mt} = G\mathbf{\Theta}_{Dt} + \epsilon_t \ , \quad \epsilon_t \sim N[\mathbf{0}, \Sigma_t] \tag{2}$$

where $G = diag(G_\theta, G_\pi, G_\rho)$ is a $(k+2)m \times (k+2)n$ interpolation matrix with G_θ, G_π and G_ρ being the spatial interpolation matrices for the components θ_M, π_M and ρ_M respectively, and $\epsilon_t = (\epsilon_{\theta t}, \epsilon_{\pi t}, \epsilon_{\rho t})'$ is the $(k+2)m$-dimensional vector of interpolation errors with components $\epsilon_{\theta t} = (\epsilon_{\theta 1t}, \ldots, \epsilon_{\theta mt})'$, $\epsilon_{\pi t} = (\epsilon_{\pi 11t}, \ldots, \epsilon_{\pi k1t}, \ldots, \epsilon_{\pi kmt})'$, $\epsilon_{\rho t} = (\epsilon_{\rho 1t}, \ldots, \epsilon_{\rho mt})'$, ϵ_{cit} $(c = \theta, \pi, \rho)$ being the interpolation error associated with component c at site i and time t. ϵ_t is assumed normally distributed with zero mean vector and covariance matrix $\Sigma_t = diag(\Sigma_{\theta t}, \Sigma_{\pi t}, \Sigma_{\rho t})$ where for each component c $(c = \theta, \pi, \rho)$, Σ_{ct} has an element $\sigma_{I_cijt} = cov(\epsilon_{cit}, \epsilon_{cjt})$ being the covariance between the interpolation error associated with component c at site i, ϵ_{cit} and ϵ_{cjt} at time t. The dimension of Σ_t is $m(k+2) \times m(k+2)$.

The *time evolution equation* is

$$\mathbf{\Theta}_{Dt} = H_t\mathbf{\Theta}_{Dt-1} + \omega_t \ , \quad \omega_t \sim N[\mathbf{0}, W_t] \tag{3}$$

where $H_t = diag(H_{\theta_{Dt}}, H_{\pi_{Dt}}, H_{\rho_{Dt}})$ is the $n(k+2) \times n(k+2)$ time evolution matrix with component sub-matrices $H_{\theta_{Dt}}$, $H_{\pi_{Dt}}$ and $H_{\rho_{Dt}}$ accounting for isotopic decays in time of each of the three components of the HBST model. $\omega_t = (\omega_{\theta_{Dt}}, \omega_{\pi_{Dt}}, \omega_{\rho_{Dt}})'$ is the $n(k+2)$-dimensional vector of time evolution errors, assumed normally distributed with zero mean vector and covariance matrix $W_t = diag(W_{\theta t}, W_{\pi t}, W_{\rho t})$ where, for each c $(c = \theta, \pi, \rho)$, W_{ct} has an element $w_{cijt} = cov(\omega_{cit}, \omega_{cjt})$ being the covariance between the time evolution error associated with component c, at site i, ω_{cit}, and ω_{cjt} at time t. Similarly to H_t, W_t is a $n(k+2) \times n(k+2)$ matrix.

The deterministic component of the system variables related to their evolution in time is described by the time evolution matrix H_t in equation (3) which associates $\mathbf{\Theta}_{Dt}$ with $\mathbf{\Theta}_{Dt-1}$. Note that this association is indirectly carried out to the off-grid measuring sites through the interpolation equation (2).

The initial values, at $t = 0$, of the mean vector $\mathbf{a}_0$ and the covariance matrix R_0 of the normal distribution of $\mathbf{\Theta}_0$ conditional on any initial information must be provided

before the model can be used. Also, initial values for the covariance matrices Σ_t and W_t in equations (2) and (3) respectively, will have to be fixed a priori by the user as we shall see in Section 4. Note that, given the measurements of instantaneous air concentrations and amount of rainfall, the diagonal forms of the matrices above can be justified by the conditional independence statement (a) drawn from the DAG of Figure 1 in the previous section.

In this paper, we investigate two cases concerning the observational covariance matrix V_t in equation (1). In the first case, V_t is assumed *known* and has its values fixed at each time step. In fact, the *known* V_t will have elements with certain fixed functional forms as we shall see in the following subsection. In the second case, V_t is assumed *unknown* and has a prior inverse-Wishart distribution attributed to it as can be seen in Subsection 2.5. The first case leads to the conjugate normal model while the second case leads to the conjugate normal-inverse-Wishart model. The prior-to-posterior updating algorithms for the normal and the normal-inverse-Wishart models are described in Appendices A and B respectively. Those algorithms are extensions of the temporal Kalman filter and of Barbosa and Harrison (1992) approximate conjugate method to include the spatial components defined above.

We can now define each of the three HBST model that are used in the application Section 4.

2.4 The HBST models with fixed functional spatial covariances

Despite the existence of a large number of functional covariance forms available for the elements of a valid (i.e. positive semi-definite) spatial covariance matrix, we have chosen two particular forms to define two variations of the HBST model. One has an exponential form proposed by Cressie (1993) and the other has a spherical form proposed by Schlather (1999) as described below. We have chosen those models for pragmatic reasons as they are not only simple to implement but also flexible to use as the parameter of spatial decay they have can be changed with the change of a single parameter.

We call *exponential hierarchical Bayesian space-time* (EHBST) model, the HBST model defined by equations (1), (2) and (3) where each component sub-matrix V_{ct} ($c = Z_D, P_D, Q_D$) of the observational covariance matrix V_t in equation (1) has elements $v_{c_{ij}t}$ ($i = 1, \ldots, m$ and $j = 1, \ldots, n$) given by

$$v_{c_{ij}t} = v_{c_it}^2 \exp(-\eta_{c_{ij}t} d_{ij}) \tag{4}$$

where $v_{c_it}^2$ is the variance at site i associated with component c at time t, $\eta_{c_{ij}t} > 0$ is a

scalar reflecting the strength of the spatial decay in the covariance, and d_{ij} is the distance between sites i and j. In this model, the spatial correlations between sites i and j decrease exponentially as the distance d_{ij} between them increases. The rate of exponential decrease is larger for larger values of the spatial decay parameter $\eta_{c_{ij}t}$ which values must be fixed by the user.

Alternatively, we call *spherical hierarchical Bayesian space-time* (SHBST) model, the HBST model defined by equations (1), (2) and (3) where each component sub-matrix V_{c_t} ($c = Z_D, P_D, Q_D$) of the observational covariance matrix V_t in equation (1) has elements $v_{c_{ij}t}$ ($i = 1, \ldots, m$ and $j = 1, \ldots, n$) given by

$$v_{c_{ij}t} = v_{c_it}^2 \left(1 - \frac{3}{2}h_{ij} + \frac{1}{2}h_{ij}^3\right) \tag{5}$$

where $v_{c_it}^2$ is the variance at site i associated with component c at time t and $h_{ij} = \frac{d_{ij}}{d_{max}}$ ($0 \leq h_{ij} \leq 1$) with d_{max} being the largest distance in the set of all underlying distances d_{ij}. In this model, the spatial correlation function is a polynomial function of order 3 of the distance d_{ij}. The spatial correlations decrease almost linearly with increases in the distances up to a certain value after which the decrease is almost exponential.

Note that compared to the EHBST, the SHBST model is a little less flexible in that the spatial smoothness depends on the distance between the two underlying sites.

In both models, the sub-matrices $V_{Z_{Dt}}$, $V_{P_{Dt}}$ and $V_{Q_{Dt}}$ of V_{Dt} have elements of the form above. They also have the sub-matrices $V_{Z_{Mt}}$, $V_{P_{Mt}}$ and $V_{Q_{Mt}}$ of V_{Mt} diagonal with fixed variances.

Note that the interpolation matrix G in (2) must be specified a priori together with the initial values, at time $t = 0$ (before any observation is taken), of the time evolution matrix H_0 in (3) and the observational, the interpolation and the time evolution covariance matrices V_0, Σ_0 and W_0 respectively. Further to those, the mean vector, $\mathbf{a}_0$, and the covariance matrix, R_0, of the Gaussian prior distribution for the initial parameter vector $\mathbf{\Theta}_0 = (\mathbf{\Theta}_{D0}, \mathbf{\Theta}_{M0})'$ must also be specified for both the EHBST and the SHBST models. After those values are fixed, data assimilation and the Bayesian sequential prior-to-posterior updating for those models are performed with the use of the extended Kalman filter algorithm described in Appendix A.

2.5 The normal inverse-Wishart HBST model

The third version of the HBST model we adopt in this paper is the *normal-inverse-Wishart* HBST (NWHBST) model which attributes a normal prior distribution with parameters

$\mathbf{a}_t$ and R_t to $\mathbf{\Theta}_t$ conditional on V_t and $\mathbf{I}_{t-1}$, i.e. $(\mathbf{\Theta}_t|\, V_t, \mathbf{I}_{t-1}) \sim N[\mathbf{a}_t, R_t]$, and a prior inverse-Wishart distribution with d_{t-1} degrees of freedom and scale matrix Ψ_{t-1} to the uncertain V_t conditional on $\mathbf{I}_{t-1}$, i.e. $(V_t|\mathbf{I}_{t-1}) \sim IW[\Psi_{t-1}, d_{t-1}]$ where IW indicates an inverse-Wishart distribution. The joint distribution of $(\mathbf{\Theta}_t, V_t|\mathbf{I}_{t-1})$ is then a normal-inverse-Wishart model, i.e. $(\mathbf{\Theta}_t, V_t|\mathbf{I}_{t-1}) \sim NIW[\mathbf{a}_t, R_t, \Psi_{t-1}, d_{t-1}]$. See e.g. Theorem 7.7.3 in Anderson (1984).

In this paper we have adopted an extension of the prior-to-posterior updating approach proposed by Barbosa and Harrison (1992) for the temporal multivariate DLM to include the spatial components of our model. This approach avoids the pragmatic problem usually caused by numerical computations involving matrices of possibly obtaining posterior covariance matrices that are not positive semi-definite and symmetric. Barbosa and Harrison approach is an approximate conjugate procedure that considers all covariance matrix factorization based on eigenvalue decomposition and (unlike the use of Cholesky decomposition) is invariant to permutations of the elements of $\mathbf{Y}_t$. It has also shown to improve on other filters such as the Robust filter introduced by Masreliez (1975) and used by West (1982) as an approximation for the marginal posterior distribution of the state parameter vector in a multivariate DLM.

The basic approach is based on the factorisation of V_t with eigenvalue matrix Λ_t and eigenvector matrix D_t such that $V_t = D_t \Lambda_t D_t' = S_t^2$, where $S_t = D_t \Lambda_t^{1/2} D_t'$ is unique, and the setting of the initial point estimate $V_0 = S_0^2$ to act as a reference matrix. Initially, $(\mathbf{\Theta}_0|\, V_0, \mathbf{I}_0) \sim N[\mathbf{a}_0, R_0]$, where $\mathbf{I}_0$ is any initial information, and $(V_0|\mathbf{I}_0) \sim IW[\Psi_0, d_0]$ where Ψ_0 of dimension $(k+2)(m+n) \times (k+2)(m+n)$ is positive semi-definite and $d_0 \geq (k+2)(m+n)$. The initial hyperparameters $\mathbf{a}_0$, R_0, Ψ_0 and d_0 are fixed by the user. Thus, at $t = 1$, $(\mathbf{\Theta}_1|\, V_0, \mathbf{I}_1) \sim N[\mathbf{a}_1, S_0 R_1 S_0]$ and $(V_1|\mathbf{I}_1) \sim IW[\Psi_1, d_1]$. The full recursive approach is shown in Appendix B.

Note that to run the NWHBST model, apart from specifying the initial prior hyperparameters described above, the user will also need to choose the values for the parameters associated with the HBST model formulation (i.e. G, H_0, Σ_0 and W_0) as described in the previous subsections.

Now that the models we will be applying in Section 4 are defined, we proceed to describe the data object of that application, that is, the radioactive near-ground concentrations in Bavaria caused by the Chernobyl accident in April 1986.

3 The Chernobyl contamination of Bavaria

In this section, we describe in detail both the measured and the predicted near-ground radioactive contamination of Bavaria caused by the Chernobyl disaster. The measurements were taken from 13 fixed monitoring stations, while the predictions were those from a long range atmospheric dispersion model, the K-model, for the $4,096$ points of a 64×64 grid over the Bavarian region.

According to the World Nuclear Association (WNA, 2008), Chernobyl's nuclear accident on the 26 April 1986 released an estimated 14 EBq (i.e. 14×10^{18} becquerels) of radioactivity to the atmosphere during a period of at least nine days. Half of the released radioactivity was of biologically inert noble gases. Most of the released material was deposited as dust and debris near Chernobyl, but lighter materials, like the six isotopes described below that were used in our application, were carried by wind over Ukraine, Belarus, Russia, Scandinavia and Europe, including Bavaria, in southern Germany, as we shall see in this section.

The OECD's Nuclear Energy Agency (NEA, 2002) stated that initial assessment of releases made by Soviet scientists based on sampling from material deposited in the former Soviet Union, estimated that all of the core inventory of biologically inert noble gases was released, and between 10 and 20% of iodine-131 (I131), tellurium-132 (Te132), caesium-134 (Cs-134) and caesium-137 (Cs-137). Iodine and caesium elements are of particular concern as they are known to be hazardous to human health. The I131 isotope has a short radioactive half-life (eight days), but can be transferred to humans relatively rapidly from the air and through the consumption of contaminated milk and leafy vegetables. Caesium isotopes on the other hand have relatively longer half-lives (Cs134 has a half-life of 2 years while Cs137 has 30 years). Many other less hazardous radioisotopes such as ruthenium-103 (Ru103), ruthenium-106 (Ru106) and Te132 amongst others, were also released during the accident.

Weather conditions at the time of the accident were such that only after the third day of the accident prevailing winds were in the western European direction. In fact, it was only from the 29 April 1986 that the monitoring stations in Bavaria started to read higher than normal measurements of radioactivity as we shall see.

The reader may refer to the World Nuclear Association (WNA, 2008) or to the Nuclear Energy Agency (NEA, 2002) for a more in-depth historical description of the accident and its consequences.

3.1 The radioactivity data in Bavaria

Daily data of Chernobyl's near-ground radioactivity air concentrations in Bavaria were obtained from the Bavarian regional office for environmental protection (Bayerisches Landesamt für Umweltschutz) for the period between 26 April and 10 May 1986 inclusive. The data consisted of γ-spec readings converted to measures of nuclide specific (i) instantaneous air concentrations, in units of Becquerel per cubic meter (Bq/m^3), and (ii) wet deposited activities, in Becquerel per litre (in Bq/l). Those readings were taken from 13 fixed monitoring stations covering the Bavarian region with an area of approximately $70,549\ Km^2$ as shown in Figure 2. Figure 2 also shows the 64×64 regular grid covering the whole Bavaria that was used by the HBST models in this application. The distance between consecutive points in the grid is 8 Km.

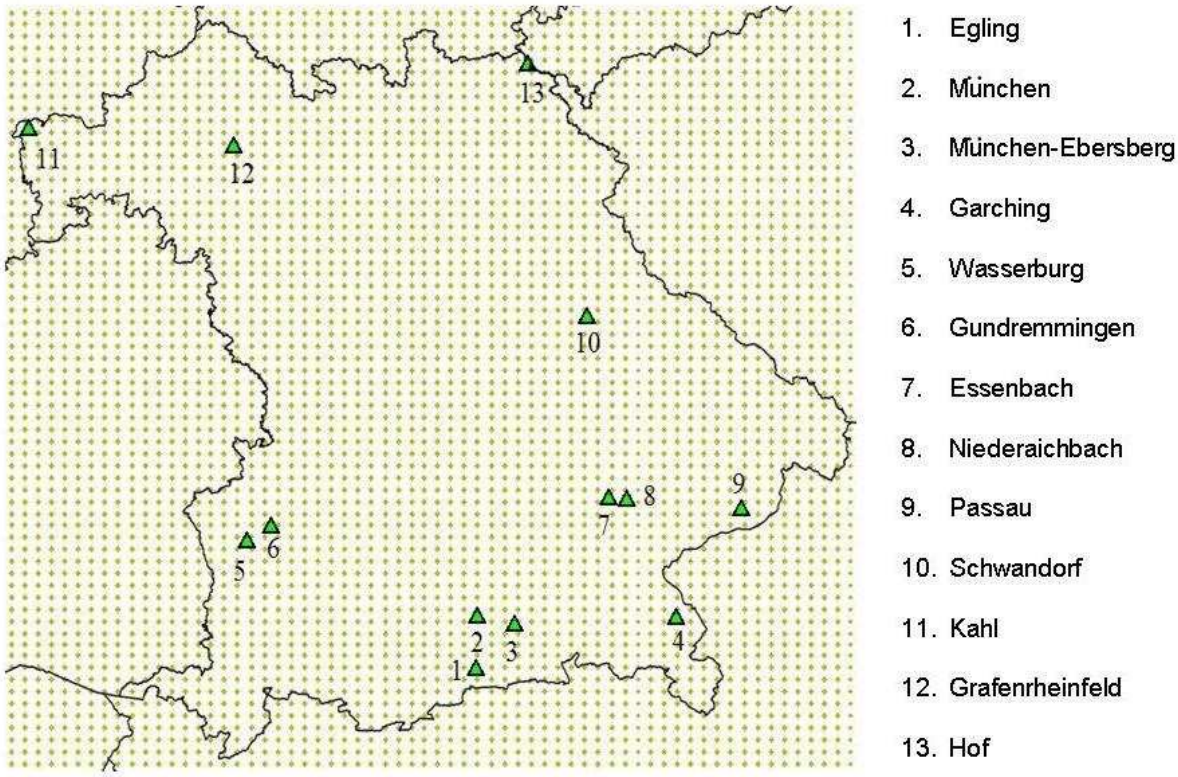

Figure 2: The map of Bavaria with the 13 fixed monitoring stations (indicated by triangles with individual numbers on the map and corresponding names on the right hand side table) and the 4096 points of the 64×64 grid over the region. The distance between consecutive grid points is 8 Km.

The data correspond to six isotopes: Ru103 and Ru106, Te132, I131, Cs134 and

Cs137. Measurements of instantaneous air concentrations were obtained for each of those six isotopes in all 13 monitoring stations, while measurements of wet depositions were only available for 5 (viz. Gundremmingen, Kahl, Ebersberg, Passau and Schwandorf) of the 13 stations.

Note that, with the exception of a few, most stations are rather scattered over the region and quite distant from one another. Most stations (9 of the 13) are located in the south of the region with the majority of those (7 of the 9) situated towards the Bavarian south-east. There is a single station in the center-east Bavaria (Schwandorf) which seems quite spatially isolated distancing by 120 Km from its nearest station (Essenbach). The northern Bavaria region has only three stations (Kahl, Grafenrheinfeld and Hof) which are located far apart from each other. The Hof station also seems quite isolated from the remaining stations. There is a large area in the center-west region with no monitoring station whatsoever. Further to those, there are about three spatial clusters of stations (München and Ebersberg, Gundremmingen and Wasserburg, and, Essenbach and Niederaichbach), all in the south, which are relatively closely located. The two nearest stations are Essenbach and Niederaichbach with a distance of approximately 10 Km separating them. The important point to note here is that there are relatively few and scattered monitoring stations to cover the region of interest.

The plots in Figure 3 show the time series of measurements of nuclide specific instantaneous air concentrations for 8 monitoring stations in the period from the 26 April to 10 May 1986. Data for the other 5 stations are not shown because near-ground concentrations at those sites were only marginally larger than the normal levels. In each plot, the time (horizontal) axis indicate the day number (we adopted $t = 1$ for 26 April, ..., $t = 15$ for 10 May 1986) and the vertical axis indicate the nuclide specific daily average air concentrations (in Bq/m^3). Also, for simplicity, the isotopes were grouped into three categories according to their levels of hazard to human health and half-lives. Thus, the less hazardous isotopes (Ru103, Ru106 and Te132) were labeled as *others* while the most hazardous were split into the shorter lived I131 with a half-life of 8 days, and the longer lived Cs134 and Cs137 with half-lives of 2 and 30 years respectively. In fact, from the radiological point of view, I131 and Cs137 are the most important radionuclides to consider for their potentially damaging health effects. The I131 radioisotope accumulates in the thyroid gland and in high doses can cause thyroid cancer while Cs137 mainly concentrates in bones and can cause leukaemia and cancer. See e.g. Castronovo (1999) and Watari *et al.* (1988) for more detailed descriptions of potential health effects of I131 and Cs137 intakes.

We can see from Figure 3 that the concentration levels for all the detected radioiso-

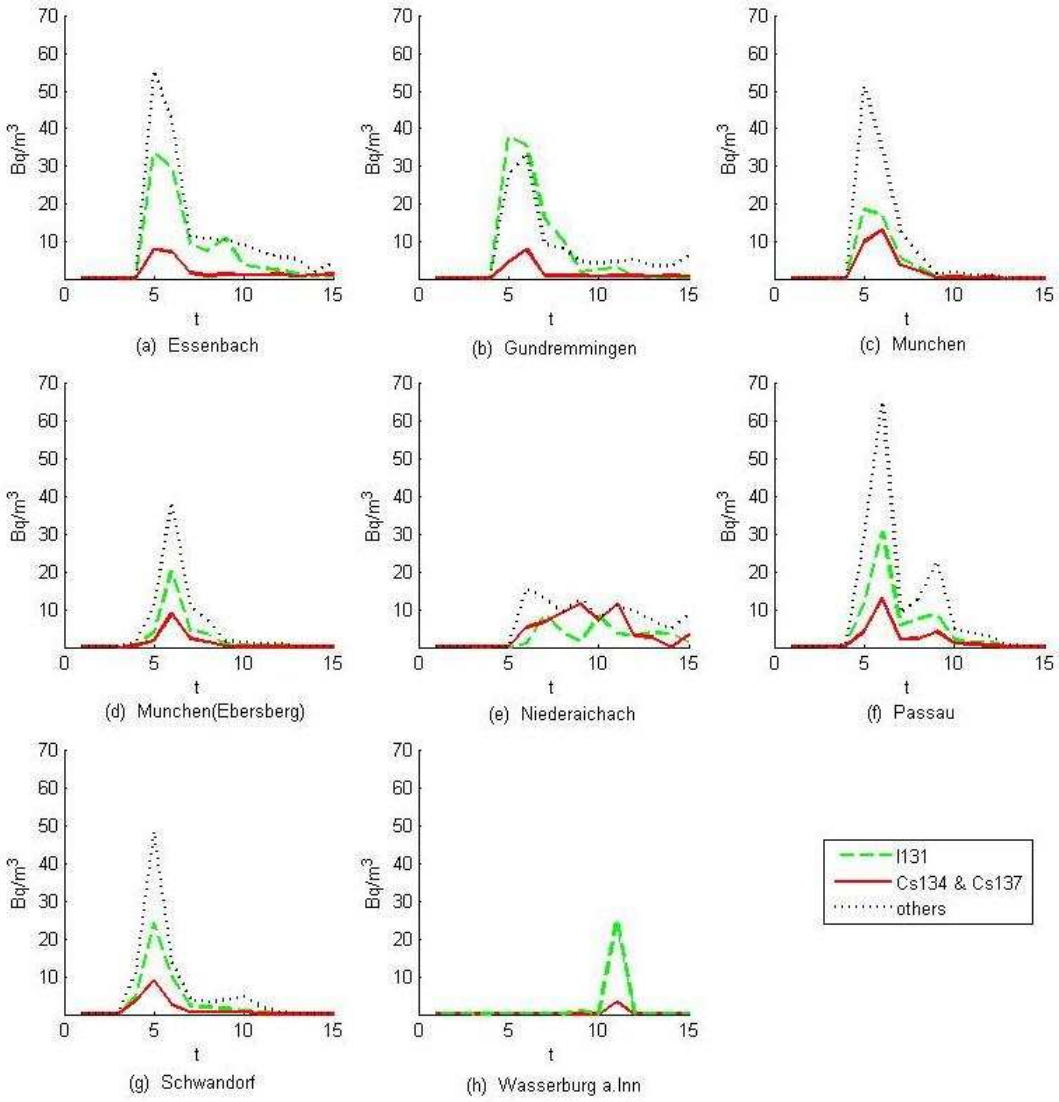

Figure 3: Daily average instantaneous near-ground air concentrations in Bq/m^3 of I131 (dashed lines), Caesium (Cs134 and Cs137, solid lines) and the other (Ru103, Ru106 and Te132, dotted lines) radioisotopes from the 26 April ($t = 1$) to the 10 May 1986 ($t = 15$) at (a) Essenbach, (b) Gundremmingen, (c) München, (d) Ebersberg, (e) Niederaichbach, (f) Passau, (g) Schwardorf, and (h) Wasserburg

topes at most stations increased dramatically from their normal background levels of $0.012 Bq/m^3$ on average before and in the early days of the accident (from $t = 1$ to $t = 4$) to much higher levels (in the range from 10 to 50 Bq/m^3) in the period from t=5 to t=10, i.e. from the fourth to the ninth day after the reactor's explosion.

Figure 4 shows for each day from the 29th of April to the 4th of May 1986, the nuclide specific near-ground radioactivity air concentrations measured at each of the 13 monitoring stations for the three isotope groups: iodine (I131), caesium (Cs134 and Cs137) and others (Ru103, Ru106 and Te132). Notice that both on the 30th April 1986 and on the 1st May 1986, the concentration levels of all isotopes were not only much higher than at any other day but also were particularly so at the monitoring stations mainly located in the south-eastern and central Bavaria (Essenbach, Gundremmingen, München, Passau and Schwandorf). In general, the more hazardous isotopes (iodine and caesium) seemed to constitute about 50% of the total concentrations with the proportions of Iodine being almost always much larger than the caesium. Also, note that the total daily concentrations had been at their natural average levels (i.e. 0.012 Bq/m^3 or less) up to the 30 April 1986 when the total levels increased enormously to approximately 36.859 Bq/m^3 in average (that is, about 3071 times the natural average level).

The meteorological conditions at Chernobyl together with the varying characteristics of the release led to a complex pattern of atmospheric transport and ground deposition both within the Soviet Union and in other countries. However, the rise in concentration levels on the fourth and fifth days after the accident is consistent with the fact, reported by the NEA (2002), page.44, that "initially the wind was blowing in a Northwesterly direction and was responsible for much of the deposition in Scandinavia, the Netherlands and Belgium and Great Britain. Later the plume shifted to the South and much of Central Europe, as well as the Northern Mediterranean and the Balkans, received some deposition, the actual severity of which depended on the height of the plume, wind speed and direction, terrain features and the amount of rainfall that occurred during the passage of the plume."

3.2 The long range atmospheric dispersal K-model

The K-model, proposed by Lauritzen and Mikkelsen (1999), is a long range atmospheric transport model of radionuclides that we have chosen, for its simplicity and good performance in real (Chernobyl accident) and simulated applications (Lauritzen *et al.*, 2006), to adopt in our application. It produces estimates of instantaneous daily average radioactive concentrations for the grid points over Bavaria (transported from Chernobyl).

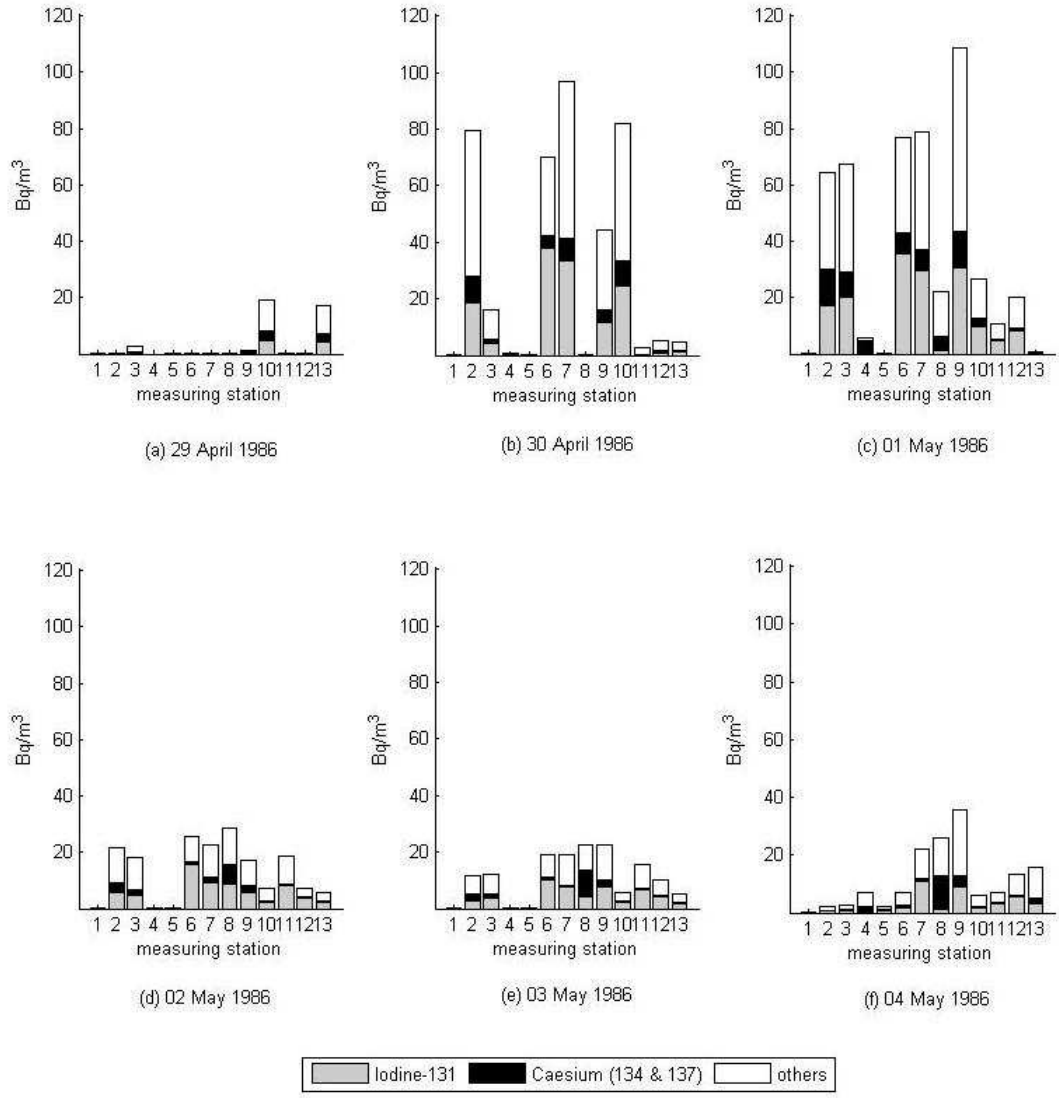

Figure 4: Near-ground daily average air concentrations of iodine (I131), Caesium (Cs134 and Cs137) and other less hazardous isotopes (Ru103, Ru106 and Te132) from the 29 April ($t = 4$) to the 4 May 1986 ($t = 9$) at each of the 13 monitoring stations in Bavaria: 1. Egling, 2. München, 3. München-Ebersberg, 4. Garching, 5. Wasserburg, 6. Gundremmingen, 7. Essenbach, 8. Niederaichbach, 9. Passau, 10. Schwandorf, 11. Kahl, 12. Grafenrheinfeld and 13. Hof.

The K-model is a first order approximation of a two-dimensional advection-diffusion process which relates turbulent fluxes to the gradient of the mean concentration in the long-range dispersion of a pollutant. In fact, the K-model describes the isotropic diffusion of the near-ground mean radioactivity concentration c_{air} for a radionuclide j at a location $\mathbf{s}$ at time t, in Bq/m^3, by the following equation:

$$c_{air}(j, \mathbf{s}, t) = \frac{\Gamma \Delta_t}{2\pi K} e^{-\frac{d(\mathbf{s}) v_{t-h}}{2K}} K_0(d^*_{j\mathbf{s}}) \tag{6}$$

where $d(\mathbf{s})$ is the distance, in Km, from location $\mathbf{s}$ to the source of release; Δ_t is the total radioactivity, in Bq, released from the nuclear reactor at time t; K is the large-scale eddy diffusivity coefficient, in m^2/s; Γ is the ensemble total activity removal rate (or "effective scavenging coefficient"), in s^{-1}; $v_{t-h(\mathbf{s})}$ is the average wind speed at time $t-h$ at the source of release ($h(\mathbf{s})$ is the length of time the radioactive plume takes to reach the location $\mathbf{s}$ where the concentration is being estimated), in m/s; and, $K_0(d^*_{j\mathbf{s}})$ is the zero-order modified Bessel Function at $d^*_{j\mathbf{s}} = (d(\mathbf{s})/2K)\sqrt{4K\Gamma + \nu_j^2}$, where ν_j is the deposition velocity, in m/s, for isotope j (assumed constant for each radionuclide). Please refer to Lauritzen and Mikkelsen (1999) for more details.

The parameters K and Γ account for a suitably chosen ensemble of long-range weather patterns and are estimated with the use of numerical weather prediction model data. In our application, we have adopted the values $K = 10^6 m^2 s^{-1}$ and $\Gamma = (1/864000)s^{-1}$ (corresponding to $10 days)^{-1}$) adopted by Lauritzen and Mikkelsen (1999) for the Chernobyl accident. Furthermore, we have determined, for each day, the average wind speed by projecting the prevailing wind vector at Chernobyl, given by Böllmann *et al.* (1987), in the southwest line towards Bavaria. The prevailing wind directions at Chernobyl in period from 26 to 29 of April 1986 were mainly pointing northwest and north towards Belarus, Scandinavia and Russia. From the 30 April, those changed direction and started to point southwest and south towards Western Europe. However, despite the wind blowing north-northwesterly initially, the average wind speeds during that period were highest so that the projected speed towards Bavaria peaked at $6.21 m/s$ ($22.37\ Km/h$) on the 26 April and fluctuated at around $4.23 m/s$ ($15.24\ Km/h$) during the following 5 days. From the 1 May, the projected wind speed dropped steadily from $4.29 m/s$ ($15.43\ Km/h$) to its minimum value of $1.18 m/s$ ($4.26\ Km/h$) on 6 May 1986. It peaked again on the 7 May to reach $5.90 m/s$ ($21.25\ Km/h$). As the releases from Chernobyl were taking about three days to reach Bavaria, we have set $h(\mathbf{s}) = 3$ in equation (6).

We have also adopted the estimated daily releases for I131, Caesium and the other isotopes from the nuclide specific estimated total releases provided by the Nuclear Energy

Agency (NEA, 2002) report and from the daily release fractions given in ApSimon *et al.* (1989). Those values were used to obtain Δ_t in (6) above.

In fact, according to the Nuclear Energy Agency (NEA, 2002), Chernobyl's accident estimated total radioactive release of I131, Caesium and the other radioisotopes (Ru103, Ru106 and Te132) together during the whole accident was in excess of 3.29 EBq. Also, ApSimon *et al.* (1989) estimated the daily percentages from the total release as 23.90%, 7.97%, 6.97%, 4.98%, 3.98%, 3.98%, 7.97%, 9.96%, 13.95% and 15.94% for each respective consecutive day in the period from 26 April to 5 May 1986, as well as 0.20% for both 6 and 7 May 1986.

The shortest distance between Chernobyl's border and its nearest point in the grid over Bavaria is 1875km. The distances used in equation (6) for other points in the grid considered the 8 Km distances between consecutive grid points. Those distances together with the values of the variables described above where used to determine the daily near-ground air concentrations estimated by the K-model at the grid points.

Because the K-model is a long range dispersal model and does not account for local atmospheric variables, the distribution of its estimated daily concentrations was rather smooth in space. This smoothness had a detrimental effect in the HBST models which produced confidence intervals for the estimated concentrations which were larger near measuring sites than at grid points. In order to produce more realistic estimates which also produced a less smooth spatial distribution of the estimated concentrations, we have made use of precipitation data (amount of rainfall) at 24 locations in Bavaria during the underlying period of time. Daily average washout measures for 24 locations in Bavaria, obtained from tutiempo.net (2008), were converted into proportions of total washouts, spatially interpolated to grid points and applied to the values estimated by the original K-model to produce what we call *corrected* K-model estimates. Those corrected daily radioactivity concentrations were then used by the HBST models.

The predicted grid-point concentrations, interpolated to the 13 off-grid monitoring sites, showed to be consistent with the measured values at those sites. In fact, those interpolated predictions gave values which were significantly closer to the observed concentrations than interpolations from the K-model's estimations alone (without the washout correction). The corrected predictions produced a *square-Root of the spatial Average of the Mean Square Errors* (RAMSE) of 10.32 Bq/m^3 that was 63.30% lower than the K-model alone. The RAMSE is calculated by

$$RAMSE = \sqrt{\frac{1}{m}\sum_{i=1}^{m}\left(\frac{1}{\tau}\sum_{t=1}^{\tau} e_{it}^2\right)}$$

where m is the total number of monitoring stations, τ is the total number of release days and e_{it} is the estimation (or prediction) error by the underlying model at site i and time t. This measure of performance is adopted by the various applied models in the following section. In this section, it was used to measure the estimation performance of the corrected K-model when interpolated to the monitoring station sites. So, the error term e_{it} in the above equation was the difference between the daily measurement at each site and the interpolated value by the corrected K-Model estimation. When used to measure the predictive performances of the HBST models, the error e_{it} is the difference between the observed value (i.e. either an off grid measurement or a grid point value estimated by the corrected K-model) and the underlying HBST model one-step-ahead median forecast for site i and day t (as defined in subsections A.4 and B.4 in Appendices A and B respectively).

The corrected K-model predictions of near-ground total radioactivity concentrations on the 29th of April were very low for the whole region, having varied between 3 and 4 Bq/m^3 that day. However, on the 30th of April, the corrected predictions increased to the range between 30 and 32 Bq/m^3 almost everywhere in the region (except for some rainfall gauging sites where higher precipitation measures implied slightly larger predicted values). The predictions reached their peaks on the 1st of May when they varied between 35 and 38 Bq/m^3 almost everywhere with the exception of some rainfall gauging sites in southern Bavaria where predictions reached between 40 and 43 Bq/m^3. Figure 5 shows the contour plot of the predicted Bavarian concentrations for the 1st of May. The dots on the map represent the 24 rainfall gauging sites used to correct the K-Model's predictions. Note that the plot is fairly consistent not only with the K-model's predictions which concentrations decay exponentially but slowly in space as the distance from the origin (Chernobyl) increases, but also with the corrections for rainfall which introduce changes to the regularity of the contour lines as well as to the regions near the gauging sites in the southern region where predicted concentrations were much larger than nearby regions. The local rainfall measures have indeed contributed to a less homogeneous and more realistic spatial distribution of the predicted concentrations. The actual rainfall measures were large in the southern region (average 0.66mm) and there were no rainfall in the central and northern region on 1st May 1986. In particular, München and Muhldorf (near Essenbach) had the largest rainfall (1.02mm) on 1st May 1986. In general, between 29th

April and 1st May 1986 the rainfall measures were large in the southern region only and no rainfall from center to north. On the 2nd of May there were no rainfall measurements in almost all the stations except Muhldorf and from 3rd May to 5th May there were no rain in the southern and central region except the northern region (average 0.40mm). After that, the average rainfall increases on 6th May (1.64mm) and it reaches its peak on 8th May (5.48mm) and again decreases to 0.45mm on an average between 9th and 10th May 1986. Note that, the rainfall measures come from almost all the region in Bavaria during 6th May to 10th May 1986.

On the 2nd of May the predictions dropped to the range between 13 and 14 Bq/m^3 almost everywhere and then from the 3rd to the 6th of May fell to the range between 8 and 12 Bq/m^3. From the 7th to the 10th of May, the corrected predictions were very low again ranging between 1.5 and 4 Bq/m^3 almost everywhere. Note that those predictions were all consistent with both the accident's dispersal behavior and the measurements described in the previous Section.

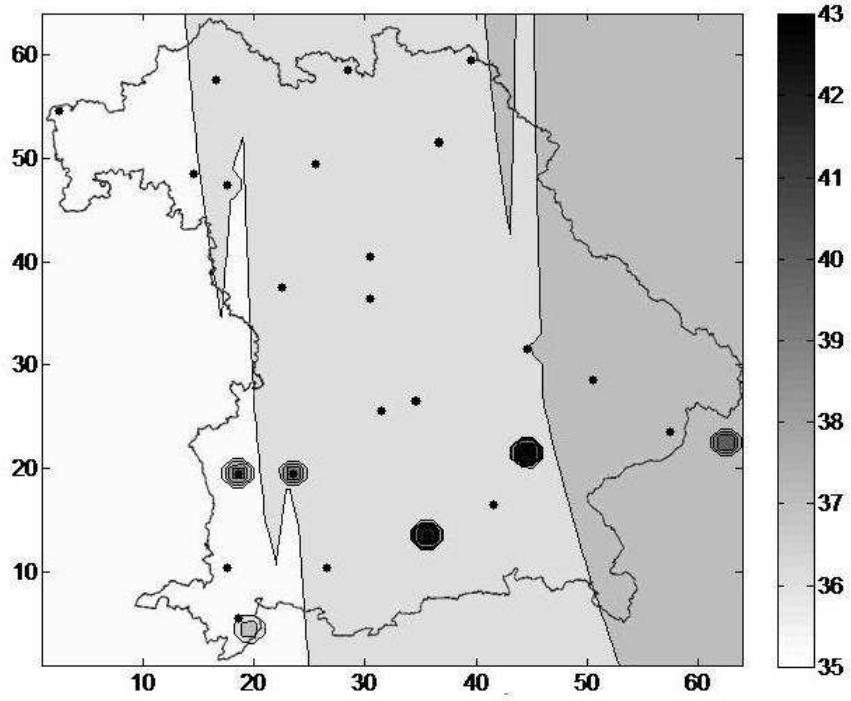

Figure 5: Contour plot of the K-model's corrected predictions of total near-ground radioactivity concentrations for the 1st May 1986. The dots represent the locations of the 24 rainfall gauging stations which measurements were used to correct the K-model's predictions.

We can now proceed to describe the results of applying the three variations of the HBST model (viz. the EHBST, the SHBST and the NWHBST models described in Section 2) using the rainfall corrected predictions from the K-model described above, to the Chernobyl's near-ground radioactivity concentrations in Bavaria described in subsection 3.1.

4 The HBST models applied to the Bavarian radioactivity concentration data

This section describes the main results of the application of the three HBST models, defined in Section 2, to the radioactive near-ground concentrations in Bavaria caused by the Chernobyl accident, presented in Section 3. Nuclide specific predictions of near-ground concentrations are made for some of the main urban areas in Bavaria for each of the three isotope groups (I131, Cs134-137 and others) defined earlier. Those are compared with observed (or interpolated for unmonitored locations) values at those urban areas on the days the concentrations were highest to assess the best predictive model. One of the aims of the analysis presented in this section is to illustrate the potential usefulness of the HBST models, in particular the NWHBST, were they to be adopted at the time of the accident.

Subsection 4.1 introduces the values chosen for the input parameters as well as the hyperparameters of the prior distributions associated with the HBST models. Subsection 4.2 shows a comparative analysis of the three models in terms of their predictive performances for both one-day-ahead (we call 'short' term) as well as for three-days-ahead ('medium' term) forecasting of total near-ground radioactivity concentrations in Bavaria. Contour plots of one-day-ahead predictions of total near-ground radioactivity concentrations and their related uncertainties are also shown for a spatial comparison of the predictive outcomes by all three models. Also, bar charts of the nuclide specific concentrations at the measuring sites predicted by the best predictive model, the NWHBST, are shown and compared with the similar bar charts of the measurements displayed in Figure 4. Further to those, one-day-ahead forecasts of nuclide specific concentrations are produced by the NWHBST model for five of the largest cities in Bavaria for the 30th April and the 1st May 1986 (the days of highest observed concentrations in Bavaria).

4.1 The input parameters of the HBST models

In our application, we have chosen an exponential form for the elements of G, such that $g_{ij} = \alpha_{ij} \exp(-\beta_{ij} d_{ij})$ for $j \in Ne(i)$ (where $Ne(i)$ denotes the set of nearest adjacent grid points to i) and $g_{ij} = 0$ for $j \notin Ne(i)$. α_{ij} is the proportionality constant such that $\sum_j g_{ij} = 1$ and $\beta_{ij} \geq 0$ is the rate of exponential interpolation decay with the distance d_{ij}. Note that this choice is fairly reasonable in applications (like ours) where not only the involved distances are considerably large (as we shall see) but also usually non-uniform meteorological conditions are largely influential. The adopted exponential form allows the choice of differing spatial decay rates to reflect particular spatial influences at distinct locations in the underlying region for every component of the HBST model. Those could be chosen for example by experts to reflect prevailing terrain structures at those locations.

Notice that for $t = 1, 2 \ldots \tau$, from the conditional independence statement (a) in subsection 2.2, we can set $V_{Dt} = diag(V_{Z_{Dt}}, V_{P_{Dt}}, V_{Q_{Dt}})$ and $V_{Mt} = diag(V_{Z_{Mt}}, V_{P_{Mt}}, V_{Q_{Mt}})$, where $V_{Z_{Dt}}$, $V_{P_{Dt}}$, $V_{Q_{Dt}}$ and $V_{Z_{Mt}}$, $V_{P_{Mt}}$ $V_{Q_{Mt}}$ are the covariance matrices of the observational errors associated with the HBST model components Z, P_j and Q for grid points and monitoring station sites respectively. Note that, the sub-matrices of V_{Dt} are not diagonal themselves, but (due to the Markovian structure of our model) those of V_{Mt} are.

The input parameters required for the observation equation (1) are $V_{Dt} = diag(V_{Z_{Dt}}$, $V_{P_{Dt}}, V_{Q_{Dt}})$ and $V_{Mt} = diag(V_{Z_{Mt}}, V_{P_{Mt}}, V_{Q_{Mt}})$. For the EHBST and the SHBST models, the variances $v^2_{c_i}$ of V_{Dt} in (4) were estimated from the available data to give $v^2_{Z_{Di}} = 1.0385$, $v^2_{P_{1Di}} = 0.0011$, $v^2_{P_{2Di}} = 0.0001$, $v^2_{P_{3Di}} = 0.0005$ for iodine, caesium and others (subscripts 1, 2 and 3 respectively) and $v^2_{Q_{Di}} = 1.8026$ for all sites i. Similarly, each component of V_{Mt} was estimated from the data to give $v^2_{Z_{Mi}} = 9.5283$, $v^2_{P_{1Mi}} = 1.9329$, $v^2_{P_{2Mi}} = 2.7459$, $v^2_{P_{3Mi}} = 6.9204$ and $v^2_{Q_{Mi}} = 17.4571$ for all sites i. The values of $\eta_{c_{ij}t}$ for the EHBST model in equation (4) were estimated from the observed data and for simplicity adopted independently of spatial location as $\eta_{c_{ij}t} = 0.0189$ for all c, i, j, t. The distance d_{max} in equation (5) in this case is the largest distance between grid points, i.e. $d_{max} = 712.76$Km. So, the covariance matrix $V_{Z_{Dt}}$ for the EHBST and the SHBST models have elements $v_{Z_{Dij}t} = 1.0385 \exp(-0.0189 d_{ij})$ and $v_{Z_{Dij}t} = 1.0385(1 - 0.0021 d_{ij} + 1.3808 \times 10^{-9} d^3_{ij})$ respectively.

In our application all the initial values of the variances described above were estimated from the data. But at the time of an accident it would not be possible to get the real data. So, in real situation those initial values would be estimated from simulation.

The components of the interpolation error vector $\epsilon_t = (\epsilon_{\theta t}, \epsilon_{\pi t}, \epsilon_{\rho t})'$ are assumed to be mutually independent such that $\Sigma_t = diag(\Sigma_{\theta t}, \Sigma_{\pi t}, \Sigma_{\rho t})$. The covariance matrices

$\Sigma_{\theta t}, \Sigma_{\pi t}$ and $\Sigma_{\rho t}$ are associated with their respective component parameter (θ, π and ρ respectively). In our application, for each component c ($c = \theta, \pi, \rho$) we have set values of the diagonal elements as

$$\sigma^2_{cit} = \sigma^2_{ct} d^*_i \tag{7}$$

where, at each time t, σ^2_{ct} is a common fixed interpolation variance associated with the component c and $d^*_i = \frac{d_i}{|d^*_{max}|}$, with d_i being the distance of the monitoring station point i ($i = 1, \ldots, m$) to its nearest grid point and d^*_{max} being the largest distance over all distances from off-grid points to their nearest grid points.

The input parameters in equation (2) are $G = diag(G_\theta, G_\pi, G_\rho)$ and $\Sigma_t = diag(\Sigma_{\theta t}, \Sigma_{\pi t}, \Sigma_{\rho t})$. For simplicity, we have adopted for all three models (independently of spatial location) a common value for the spatial decay parameters $\beta_{ij} = \beta = 0.2$ for all i, j. Also, for simplicity, the values of α_{ij}, for the elements $g_{ij} = \alpha_{ij} \exp\{-\beta_{ij} d_{ij}\}$ of all the submatrices of G, were set to be α_i for all $j \in Ne(i)$. Those values of α_i for $i = 1, 2 \ldots 13$ were estimated from the observed data based on the assumption that $\sum_j g_{ij} = 1$ for all $j \in Ne(i)$ to give $0.73, 0.98, 0.63, 0.78, 1.34, 0.53, 0.77, 0.77, 0.76, 0.76, 0.73, 0.74$ and 0.76 for $i = 1, \ldots, 13$ respectively.

Each submatrix Σ_{ct} ($c = \theta, \pi, \rho$) of Σ_t is also diagonal with elements σ^2_{cit} as in equation (7). A common value $\sigma^2 = 8.46 \times 10^{-7}$ (estimated from data) was chosen for σ^2_{cit} for all c, i and t. For each i, $d^*_i = \frac{d_i}{d^*_{max}}$ with $d^*_{max} = 10.21$Km.

At each time t, the decay associated with the total deposited activity consists of the aggregation of each deposited radionuclide's decay from the time of the initial deposition. Thus, the sub-matrix $H_{\theta_{Dt}}$ will be diagonal with each diagonal element $h_{\theta_{Dt}} = \sum_j^k h_{D_{jt}}$ independently of spatial location, where

$$h_{\theta_{Djt}} = \exp(-\lambda_j t) \tag{8}$$

with $\lambda_j = \frac{ln(2)}{T_{1/2}(j)}$ and $T_{1/2}(j)$ being the half-life of isotope type j, that is, the amount of time required for 50% of the radioactive atoms in a sample to undergo a radioactive (or nuclear) decay.

For practical reasons, we consider the mother-to-daughter decay of isotopes (i.e. the decay of the same element into another type of isotope) as negligible. Thus, the sub-matrix $H_{\pi_{Dt}}$ for the proportions components will be a $k \times k$ diagonal matrix with elements $H_{\pi_{Djt}}$, $j = 1, \ldots k$, where for each j, $H_{\pi_{Djt}}$ is a $n \times n$ diagonal matrix with elements $h_{\theta_{Djt}} = \exp(-\lambda_j t)$ independently of spatial location with λ_j as described above.

The sub-matrix $H_{\rho_{Dt}}$ related to the proportions of wet deposition will also be a diagonal matrix with elements $h_{\rho_{Dt}} = \exp(-\lambda t)$ independent of the spatial location with suitably chosen decay parameter λ.

The input parameters in equation (3) are $H_t = diag(H_{\theta_{Dt}}, H_{\pi_{Dt}}, H_{\rho_{Dt}})$ and the covariance matrix $W_t = diag(W_{\theta t}, W_{\pi t}, W_{\rho t})$. All the submatrices of H_t are diagonal and for each component we adopted the same diagonal values independently of spatial location. Each diagonal element of $H_{\theta_{Dt}}$ is $h_{\theta_{Djt}} = h_{\theta_D} = \sum_{i=1}^{6} \exp(-\lambda_i t)$ independently of each spatial location for all the isotope types j ($j = 1, ..., 6$). The diagonal elements of $H_{\pi_{Dt}}$ are $\exp(-\lambda_1 t)$, $\sum_{j=2}^{3} \exp(-\lambda_j t)$ and $\sum_{j=4}^{6} \exp(-\lambda_j t)$ for each group of radionuclides (e.g. iodine, caesium and others) and the each diagonal element of $H_{\rho_{Dt}}$ is $h_{\rho_{Dt}} = \exp(-\lambda t)$ with $\lambda = 0.05$ independently of each spatial locations. The value of λ is suitably fixed by the user. As the wet deposition mainly depends on rainfall, so we have chosen a quite fast exponential decay so that the effect of rainfall covers only the neighboring region of the place where rainfall happens. The diagonal elements of all submatrices of H_t are of exponential form as described in equation (8). The parameters $\lambda_j = \frac{ln(2)}{T_{1/2}(j)}$ were determined from the half-life $T_{1/2}(j)$ of each isotope type j ($j = 1, ..., 6$). The half-life values of the radioisotopes I-131, Cs-134, Cs-137, Ru-103, Ru-106 and Te-132 are 8.04, 753.72, 11033.95, 39.27, 372.3 and 3.204 days respectively. Note the relatively short half-lives of I-131 and Te-132 compared with those of Cs-134, Cs-137, Ru-103 and Ru-106.

For the EHBST and the SHBST models, the elements of each submatrix W_{ct} of W_t described in subsection 2.3 are w_{cijt}, which have fixed exponential form similar to $v_{c_{ijt}}$ described in equation (4).

Finally, for the data assimilation process by the EHBST and the SHBST models, the initial values of those models' hyperparameters, i.e. $\mathbf{m}_0$ and C_0, were fixed. The mean vector $\mathbf{m}_0$ was chosen as the average of all the grid point values independently of spatial location and the elements of the covariance matrix C_0 were chosen as an exponential form similar to $\sigma_{c_{ijt}}$ described in equation (4).

Note that for other applications those values should be suitably chosen by the user according to the initial information available. One possible choice to reflect lack of information is to adopt a non-informative prior distribution for $\mathbf{\Theta}_0$. On the other hand, when the data represents the continuation of a previously observed series, then the time origin $t = 0$ is just being an arbitrary label. In such cases, the initial prior is viewed as sufficiently summarising the information from the past, $\mathbf{\Theta}_0$ having the concrete interpretation of the final state vector for the historical data.

The NWHBST model adopted the algorithm described in Appendix B. The prior parameters at time $t = 1$ for the NWHBST model are $\mathbf{a}_1$, R_1, Ψ_0 and d_0. To obtain the values of $\mathbf{a}_1$ and R_1, we need the initial mean vector $\mathbf{m}_0$ and the initial variance-covariance matrix C_0 as described above. Ψ_0 is the initial scale matrix for the inverse-Wishart distribution. The implementation of the Barbosa and Harrison updating algorithm described in

Appendix B requires the computation of two matrix square roots as described in Section B.4 of Appendix B. Those matrix square roots were implemented in two different ways, using respectively two different matrix factorisation techniques: the Cholesky decomposition method and the eigen-value decomposition method. For the Cholesky decomposition method, Ψ_0 has to be a positive definite matrix, and for the eigen-value decomposition method, Ψ_0 should be a symmetric square matrix. In our application we chose Ψ_0 from an exponential family which guaranteed its positive definiteness. We chose the elements of the initial scale matrix Ψ_0 to have exponential forms similar to $\sigma_{c_{ijt}}$ in equation (4). The initial degree of freedom d_0 was chosen as $d_0 = (m+n) \times (k+2) = 20545$, where $m = 13$, $n = (64 \times 64)$ and $k = 3$. The matrix S_0 in the algorithm of Appendix B is the square-root of the initial observational matrix V_0, where $V_0 = \Psi_0/d_0$.

With all the input parameters and hyperparameters specified, the Chernobyl data assimilation was carried out by the EHBST and the SHBST models through the spatio-temporal Kalman filter described in Appendix A and by the NWHBST model through the updating algorithm described in Appendix B.

4.2 Predictive distributions and model's performances

The RAMSEs of all three models were computed to assess their 'short' (one-day-ahead) as well as their 'medium' term (three-days-ahead) predictive performances for the total near-ground radioactivity concentrations. That is, for each day t, the means of each model's predictive distribution of total concentrations at all underlying spatial points for days $t+1$ and $t+3$ were used to calculate the forecasting errors in the computation of the 'short' and 'medium' term RAMSEs respectively.

Figures 6(a) and (b) show the RAMSE plots for the one-day-ahead and the three-days-ahead forecasts respectively for each of the three models. Note that the NWHBST (solid line) had the best overall performance of the three models in both short and medium term forecasting. The Chernobyl contamination in Bavaria is measured from Day 4 (29th April 1986) to Day 15 (10th May 1986). So, the RAMSE for one-day ahead forecast starts from Day 5 (30th April 1986) as shown in Figure 6(a) and the RAMSE for three-day ahead forecast starts from Day 7 (2nd May 1986) as shown in Figure 6(b).

The concentration increased from practically natural levels to very high levels in the period from day 5 to day 7 for the short term, and on days 7 and 8 for the medium term forecasting, all the models' performances decreased with the RAMSE jumping to values in the range from 1.63 to 46.83 Bq/m^3 and from 20.50 to 53.19 Bq/m^3 for the short and medium respectively. However, in those periods the NWHBST produced the best relative

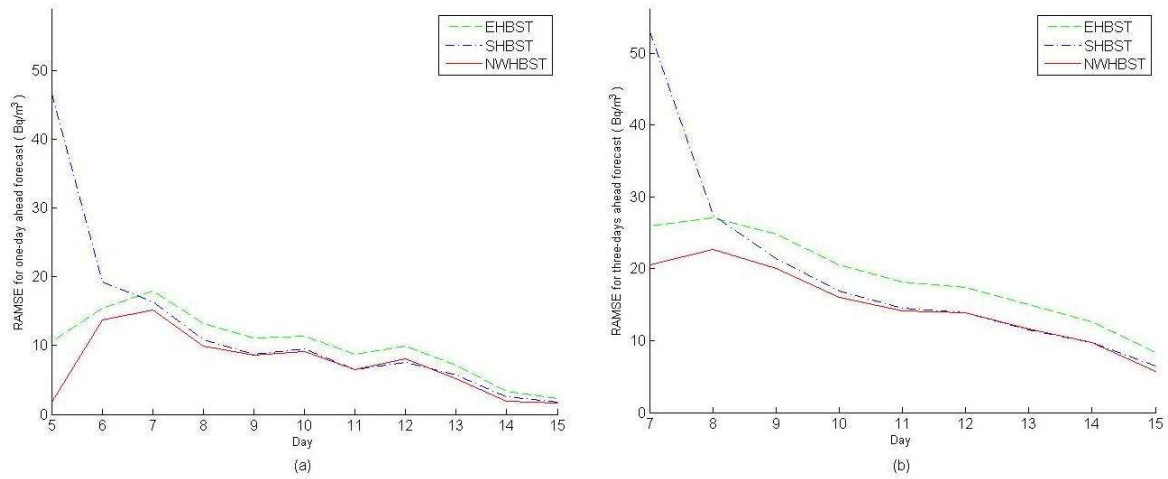

Figure 6: The RAMSE for (a) one-day ahead forecasts, and (b) three-days ahead forecasts for the EHBST (dashed line), SHBST (dash-dotted line) and the NWHBST (solid line) models.

performance of all models, with its RAMSE being on average 30.6% and 18.5% lower (for the short and the medium term periods respectively) than the second best model, the EHBST. The SHBST was the worst performing model during those periods, followed by the EHBST. In the period from day 8 to 15 and from day 9 to 15 (for the short and medium term periods respectively), all the models performances improved with their RAMSEs practically displaying a negative trend. Again, on those periods the NWHBST model slightly outperformed the remaining models. This time though the RAMSE from the NHWBST model was only 4.6% and 3.6% lower (for the short and medium term periods respectively) than the second best model, the SHBST. Overall, the NWHBST displayed the best performance on the RAMSE criteria showing average gains of 36.7% and 26.6% (for the short and medium term periods respectively) over the second best model, the EHBST.

The bar charts (a) to (f) in Figure 7 display for each day from the 29 April (day 4) to the 4 May 1986 (day 9), the one-step-ahead forecasts of near-ground radioactivity air concentrations of Iodine (I131 in grey), caesium (Cs134 and Cs137, in black) and others (Ru103, Ru106 and Te132, in white) by the NWHBST model for the sites of the 13 monitoring stations. Comparing those forecasts with the measured values shown in Figure 4, we notice that in general for each day the NWHBST model produced mixed results with under and over forecasting at some sites but also some pretty close predictions at others. For the 30 April and 1 May 1986, the predicted concentrations were a lot larger

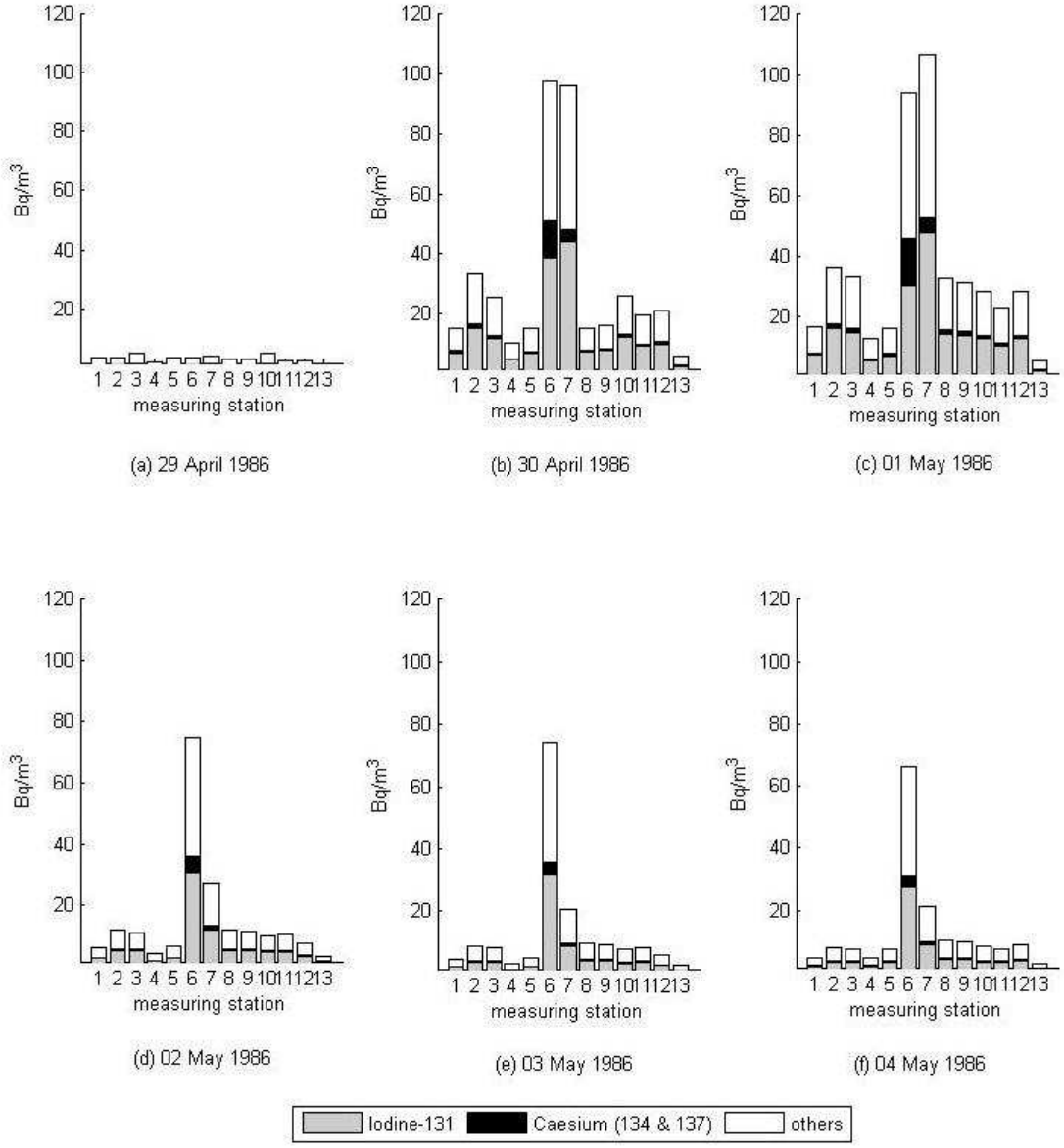

Figure 7: NWHBST model's predicted near-ground daily average air concentrations of iodine (I131), Caesium (Cs134 and Cs137) and other less hazardous isotopes (Ru103, Ru106 and Te132) from the 29 April ($t = 4$) to the 4 May 1986 ($t = 9$) at each of the 13 monitoring stations in Bavaria: 1. Egling, 2. München, 3. München-Ebersberg, 4. Garching, 5. Wasserburg, 6. Gundremmingen, 7. Essenbach, 8. Niederaichbach, 9. Passau, 10. Schwandorf, 11. Kahl, 12. Grafenrheinfeld and 13. Hof.

than on the 29 April and closer to the measured values at some sites, in particular for sites 6 and 7. This is because there were more accurate rainfall predictions near those sites. Such that, the rainfall monitoring stations Augsburg and Ingolstadt are very close to the radioactivity monitoring stations Gundremmingen (site 6) and Essenbach (site 7) respectively. Due to same reason of inaccurate rainfall information, the NWHBST model produced mixed results with under and over predictive values in some measuring sites.

Note that on day 5, the predicted level of caesium was larger than the measured at site 6 but not by a large amount, and at site 7, the predicted caesium level was smaller than the measured but again by a small amount. On day 6, the predicted level of caesium varied in a pattern similar to day 5 at the sites 6 and 7. In general at site 6, the predicted caesium level was larger than the measured but by small amounts between days 5 and 9.

The predicted levels of iodine for sites 6 and 7 were very close to the measurements on days 5 and 6. At München (site 2), the predicted level of iodine was very close to the measurements between days 5 and 9. In general, on days 5 and 6, the predicted levels of iodine were very close to the measurements at most of the measuring sites except at 1, 5 and 8.

As the average natural level of concentration for caesium was $0.0009 Bq/m^3$ and the NWHBST models' predicted level of concentrations of caesium for site 6 (Gundremmingen) and site 7 (Essenbach) were $12.49 Bq/m^3$ and $3.82 Bq/m^3$ on 30th April and $15.84 Bq/m^3$ and $4.56 Bq/m^3$ on 1st May. So the level of concentrations of caesium for sites 6 and 7 were approximately 13878 and 4244 times larger on the 30th April, and 17600 and 5066 times larger on the 1st May than the natural levels of concentration.

On the other hand, as the average natural level of concentration for iodine was $0.0009 Bq/m^3$ and the NWHBST models' predicted level of concentrations of iodine for sites 6 and 7 were $38.66 Bq/m^3$ and $44.15 Bq/m^3$ on the 30th April and $30.21 Bq/m^3$ and $47.99 Bq/m^3$ on the 1st May. So, the predicted level of concentrations of iodine for sites 6 and 7 were approximately 42955 and 49055 times larger on 30th April and 33566 and 53322 times larger on the 1st May than the natural levels of concentration.

From a decision maker's point of view, it may be important to predict the concentration levels at urban areas of larger populations. Thus, we have produced one-day-ahead predictions by the NWHBST model for the main cities in Bavaria. Table 1 shows the one-day-ahead predicted daily average air concentrations (in Bq/m^3) and the corresponding observed (or, interpolated) values for the iodine and caesium isotopes calculated on the 30th April and the 1st May 1986 at the five Bavarian cities: Augsburg, München, Ingolstadt, Nürnberg and Würzburg. To obtain the interpolated values at those cities, we adopted an interpolation rule similar to that used by the EHBST model in the previous

section but with a smaller spatial decay of 0.0189 for the exponential form of the elements of the observational covariance matrix.

The large cities and the corresponding nearest monitoring stations in parenthesis are: Augsburg (Gundremmingen), München (München), Ingolstadt (Essenbach), Nürnberg (Schwandorf), Würzburg (Grafenrheinfeld). These cities mainly cover the region of south-west (Augsburg), south (München), south-east (Ingolstadt), north-east (Nürnberg) and north-west (Würzburg) in Bavaria.

Note that, the predicted values of iodine and caesium by the NWHBST model fit well the observed (or interpolated values) shown in Table 1. The values with '$*$' marks lie outside the 95% predictive interval.

Table 1: The NWHBST model's one-day ahead predicted (pred) daily average air concentrations (Bq/m^3) and the corresponding observed/interpolated (obs/int) values (Bq/m^3) for the two groups of radionuclides (Iodine and Caesium) calculated on the 30th April and 1st May 1986 at some of the large cities (Augsburg, München, Ingolstadt, Nürnberg, Würzburg) in Bavaria.

Major	30th April 1986				1st May 1986			
Cities	Iodine		Caesium		Iodine		Caesium	
	obs/int	pred	obs/int	pred	obs/int	pred	obs/int	pred
Augsburg	31.03	31.56	3.61	10.19*	28.94	24.67	6.31	12.93*
München	3.04	11.55	1.28	1.00	15.36	12.42	6.67	1.18*
Ingolstadt	5.95	7.80	1.38	0.68	5.24	8.49	1.29	0.81
Nürnberg	2.12	1.04	0.79	0.09	0.86	1.12	0.24	0.11
Würzburg	0.26	3.15	0.25	0.27	2.62	4.18	0.36	0.39

The contour plots (a1) to (c1) in Figure 8 display the one-day ahead forecasts of the total near-ground radioactivity air concentrations in Bavaria on 01 May 1986 by the three HBST models. In all the contour plots in Figure 8, low concentrations are in white and high concentrations are in black. Intermediate values are displayed in various intensities of gray, the darker the intensity the larger the concentration values.

We noticed that in general the one-day ahead predictions varied from $300Bq/m^3$ to $350Bq/m^3$ for the EHBST model, where as for the SHBST model it reached $600Bq/m^3$ to $700Bq/m^3$ in regions near München, Passau and Regensburg, i.e. the north-east and the south-east region of Bavaria. On the other hand, for the NWHBST model, the one-day

ahead prediction varied from $50Bq/m^3$ to $150Bq/m^3$ in the same region mentioned above. Comparing those forecasts with the measured values in some monitoring stations located in that region shown in Figure 4, we notice that in general on the 1st May 1986 the NWHBST model produced better results (i.e. close to the measured values) compared to the EHBST and SHBST models. As we have seen before, the RAMSE for the one-day-ahead forecast is larger on day 5 (1st May) for the SHBST model, which can also be seen from the contour plots for one-day ahead forecasts.

The contour plots (a2) to (c2) in Figure 8 show the corresponding predictive uncertainty maps for the total near ground concentrations in Bavaria on 01 May 1986 by the three HBST models. By incorporating this information, we can greatly improve the prediction provided by the one-day ahead prediction alone. Comparing those uncertainty maps, we notice that in general on the 1st May 1986 the predictive uncertainties were larger for the EHBST model compared to other two models. The NWHBST model has the smallest uncertainty which can be seen from the lowest RAMSE for one-day ahead forecast in Figure 6(a).

Finally, we can conclude that the NWHBST model among all the HBST models that were considered performed better in the predictive sense. Still the predictions from the NWHBST model could have been improved by incorporating more accurate rainfall information over the geographic region of interest. More accurate rainfall information would produce more accurate predictions by the K-model at the grid points which, in their turn, would improve the quality of the NWHBST's predictions. In this application we had only 13 sparse measuring sites in the Bavarian region to cover an area of approximately $70,549Km^2$ as shown in Figure 2. Obviously, more measurements would contribute to better data assimilation and model performance.

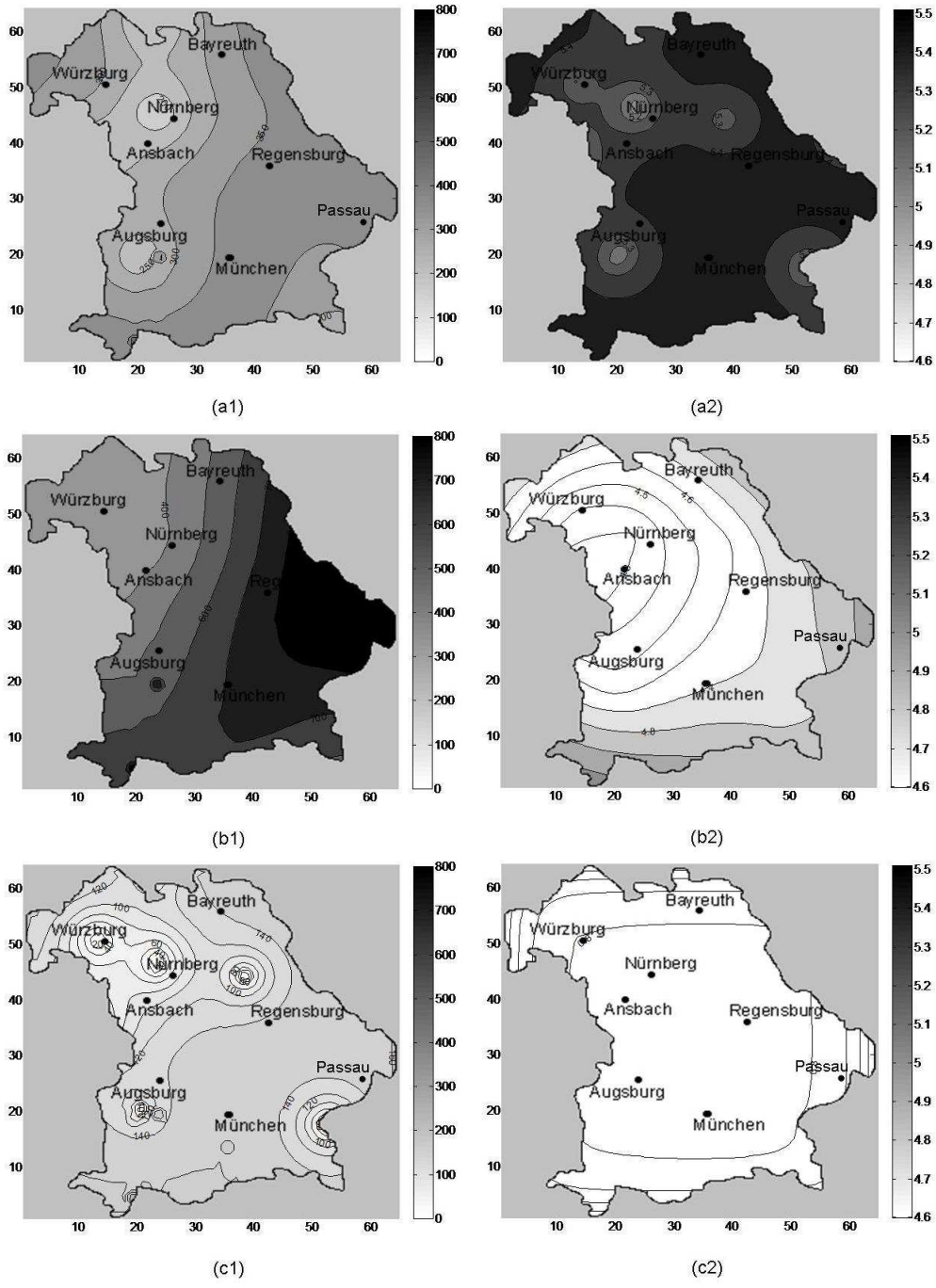

Figure 8: The one-day ahead predictive means for the (a1) EHBST, (b1) SHBST and (c1) NWHBST models and the related uncertainty maps of the one-day ahead prediction for the (a2) EHBST, (b2) SHBST and (c2) NWHBST models on 01 May 1986 (contours correspond to predictive means and the predictive standard deviation of the total near ground radioactive deposition, based on the full data set)

5 Conclusion

The HBST models proposed in this paper provide a flexible framework for modelling nuclide specific near-ground radioactive concentrations in time and space. Those models are valid for any data sets that are discrete in time and continuous in space, including data observed at irregular grids or at locations that change over time. They can be adapted for use in different countries with different measuring resources. They use predictions from a long range atmospheric dispersal model as data to produce improved estimation of concentration levels which account for weather information.

The accuracy of the HBST models depend crucially on the quality of inputs from the long range atmospheric dispersal model as this in principle accounts for atmospheric effects. Processes of the type being modelled here are meteorology dependent by nature. In our case, too smoothed predictions from the atmospheric model can lead to HBST models predictions with smaller associated uncertainties than expected being obtained. The K-model did a decent job here but other more sophisticated models such as RIMPUFF dispersion model by Mikkelsen *et al.* (1984), which explicitly accounts for atmospheric forecasts and measurements including temperature, precipitation and wind fields, are expected to perform better and thus improve the HBST models' predictive qualities.

The model formulation presented in this paper, addresses the issue of compatibility between outputs of modules in a chain system that models all the phases of the whole accident and the inputs required by other modules further down in the chain. In particular, it makes it possible to coherently transfer information (updated by measurements and/or other information) between a long range atmospheric dispersal model and a food contamination model.

An extension of the proposed HBST model to include explanatory variables is technically straightforward. It would only require the inclusion of a corresponding regression matrix in the set of the model's equations and consequently on the set of updating Kalman filter equations. Similarly, a generalization to distribution-free models (associated to processes that can be characterized by the first two moments only) on the line of Goldstein (1976) Bayes linear method would be relatively easy to implement.

Certainly a future step in our developments will consist of making use of a fully computational MCMC approach. A possible advantage of that would be a better quality of the posterior densities estimation achieved by the inclusion of the process non-linearities in the methodology. However, in this non-linear setting complications associated with unidentifiability and convergence are likely to be significant. Other possible extensions of our model include the use of anisotropic covariance functions as proposed by Sampson

and Guttorp (1992) to consider directional spatial dependencies.

Off-grid unmonitored sites of interest (such as large cities, rivers, agricultural regions, etc) could also be included in the model by augmentation of vectors and matrices only. This would allow, via model interpolation, the estimation of more accurate contamination levels at those sites.

Appendix A: A space-time extension of the Kalman filter algorithm for the HBST model

A.1 The initial information:

The distribution of $\mathbf{\Theta}_0 = (\mathbf{\Theta}_{D0}, \mathbf{\Theta}_{M0})'$ at time $t = 0$ is assumed to be a multivariate normal distribution with parameters $\mathbf{a}_0$ and R_0, that is, $\mathbf{\Theta}_0 \sim N[\mathbf{a}_0, R_0]$, where $\mathbf{a}_0 = (\mathbf{m}_0, G\mathbf{m}_0)'$ and

$$R_0 = \begin{pmatrix} C_0 & GC_0 \\ C_0 G' & GC_0 G' + \Sigma_0 \end{pmatrix}.$$

A.2 The prior distribution of $\mathbf{\Theta}_t$:

The prior distribution of $\mathbf{\Theta}_t = (\mathbf{\Theta}_{Dt}, \mathbf{\Theta}_{Mt})'$ at time t ($t = 1, 2, ...$), conditional on the information $\mathbf{I}_{t-1}$ available at time $t-1$, is given by $(\mathbf{\Theta}_t|\mathbf{I}_{t-1}) \sim N[\mathbf{a}_t, R_t]$ where $\mathbf{a}_t = (H_t\mathbf{m}_{t-1}, GH_t\mathbf{m}_{t-1})'$ and

$$R_t = \begin{pmatrix} H_t C_{t-1} H_t' + W_t & GH_t C_{t-1} H_t' + GW_t \\ \\ H_t C_{t-1} H_t' G' + W_t G' & GH_t C_{t-1} H_t' G' + GW_t G' + \Sigma_t \end{pmatrix}.$$

A.3 The one-step predictive distribution of $\mathbf{Y}_t$:

The one-step ahead predictive distribution of $\mathbf{Y}_t = (\mathbf{Y}_{Dt}, \mathbf{Y}_{Mt})'$ conditional on $\mathbf{I}_{t-1}$, is a multivariate normal distribution with mean vector $\mathbf{f}_t$ and covariance matrix Q_t, that is $(\mathbf{Y}_t|\mathbf{I}_{t-1}) \sim N[\mathbf{f}_t, Q_t]$, where $\mathbf{f}_t = \mathbf{a}_t$ and $Q_t = R_t + V_t$.

A.4 The posterior distribution of $\mathbf{\Theta}_t$:

The distribution of $\mathbf{\Theta}_t = (\mathbf{\Theta}_{Dt}, \mathbf{\Theta}_{Mt})'$ conditional on $\mathbf{I}_t = \{\mathbf{I}_{t-1}, \mathbf{Y}_t\}$ is a multivariate normal with mean vector $\mathbf{a}_t^*$ and covariance matrix R_t^*, that is $(\mathbf{\Theta}_t|\mathbf{I}_t) \sim N[\mathbf{a}_t^*, R_t^*]$ where $\mathbf{a}_t^* = \mathbf{a}_t + A_t\mathbf{e}_t$ and $R_t^* = R_t - A_t Q_t A_t'$, with $A_t = R_t Q_t^{-1}$, and $\mathbf{e}_t = \begin{pmatrix} \mathbf{Y}_{Dt} - H_t\mathbf{m}_{t-1} \\ \mathbf{Y}_{Mt} - GH_t\mathbf{m}_{t-1} \end{pmatrix}$ being the one-step-ahead forecasting error vector.

A.5 The k-step predictive distribution for $\mathbf{Y}_{t+k}$:

The k-steps ahead predictive distribution for $\mathbf{Y}_{t+k}$ given $\mathbf{I}_t$ is a multivariate normal with mean $\mathbf{f}_t(k)$ and covariance matrix $Q_t(k)$ where $k = 1, 2, ...$ That is,

$$(\mathbf{Y}_{t+k}|\mathbf{I}_t) \sim N[\mathbf{f}_t(k), Q_t(k)]$$

where $\mathbf{f}_t(k) = \mathbf{a}_t(k)$ and $Q_t(k) = R_t(k) + V_{t+k}$,
with $\mathbf{a}_t(k) = H_{t+k}\mathbf{a}_t(k-1)$ and $R_t(k) = H_{t+k}R_t(k-1)H'_{t+k} + W_{t+k}$,
where $\mathbf{a}_t(0) = \mathbf{a}_t^*$ and $R_t(0) = R_t^*$,
with $\mathbf{a}_t^*$ and R_t^* are defined in A.4.

Appendix B: The prior-to-posterior updating algorithm for the normal-inverse-Wishart HBST model

Suppose, at time t, the state parameter vector $\mathbf{\Theta}_t = (\mathbf{\Theta}_{Dt}, \mathbf{\Theta}_{Mt})'$ and the observational covariance matrix V_t are *unknown*.

B.1 The initial information:

Let, the distribution of $\mathbf{\Theta}_0 = (\mathbf{\Theta}_{D0}, \mathbf{\Theta}_{M0})'$ conditional on V_0 and on the initial information $\mathbf{I}_0$ be a multivariate normal with *fixed* and *known* hyperparameters $\mathbf{a}_0 = (\mathbf{m}_0, G\mathbf{m}_0)'$ where $\mathbf{m}_0 = (m_{D10}, \ldots, m_{Dn0}, \ldots, m_{D(k+2)n0})'$ are initial means at grid points for each component Z, P and Q, and $R_0 = \begin{pmatrix} C_0 & GC_0 \\ C_0G' & GC_0G' + \Sigma_0 \end{pmatrix}$, where C_0 of dimension $((k+2)n \times (k+2)n)$ is the initial spatial covariance matrix (similar to V_{Dt} defined in Subsection 2.3) associated with the components Z, P and Q for all the grid points.

$$(\mathbf{\Theta}_0|\, V_0, \mathbf{I}_0) \sim N\,[\mathbf{a}_0, R_0]$$

and the distribution of V_0 conditional on the initial information $\mathbf{I}_0$ is an inverse-Wishart with the *fixed* parameters $d_0 \geq (k+2)(m+n)$ and $\Psi_0 > 0$,

$$V_0|\mathbf{I}_0 \sim IW\,[\Psi_0, d_0]$$

with $V_0 = \Psi_0/d_0$.

B.2 The prior distribution of $\mathbf{\Theta}_t$:

The prior distribution of $\boldsymbol{\Theta}_t = (\boldsymbol{\Theta}_{Dt}, \boldsymbol{\Theta}_{Mt})'$ at time t $(t \geq 1)$, conditional on V_0 and the information $\mathbf{I}_{t-1}$ is given by

$$\boldsymbol{\Theta}_t | \, V_0, \mathbf{I}_{t-1} \sim N \left[\mathbf{a}_t, S_0 R_t S_0 \right]$$

and the distribution of V_t conditional on $\mathbf{I}_{t-1}$ is an inverse-Wishart with parameters $d_{t-1} \geq (k+2)(m+n)$ and $\Psi_{t-1} > 0$,

$$V_t | \mathbf{I}_{t-1} \sim IW \left[\Psi_{t-1}, d_{t-1} \right]$$

where $\mathbf{a}_t = \begin{pmatrix} H_t \mathbf{m}_{t-1} \\ G H_t \mathbf{m}_{t-1} \end{pmatrix}$ and $R_t = \begin{pmatrix} H_t C_{t-1} H_t' + W_t & G H_t C_{t-1} H_t' + G W_t \\ H_t C_{t-1} H_t' G' + W_t G' & G H_t C_{t-1} H_t' G' + G W_t G' + \Sigma_t \end{pmatrix}$

B.3 The predictive distribution of $\mathbf{Y}_t$:

The one-step ahead predictive distribution of $\mathbf{Y}_t = (\mathbf{Y}_{Dt}, \mathbf{Y}_{Mt})'$ made at time $t-1$ is a multivariate Student-t distribution with mean vector $\mathbf{f}_t$ and covariance matrix $S_{t-1} Q_t S_{t-1}$, that is

$$\mathbf{Y}_t \sim T \left[\mathbf{f}_t, S_{t-1} Q_t S_{t-1}, d_{t-1} \right]$$

where $\mathbf{f}_t = \mathbf{a}_t$. $S_{t-1}^2 = \Psi_{t-1} / d_{t-1}$ and $Q_t = I_t + R_t$, with an identity matrix I_t.

B.4 The posterior distribution of $\boldsymbol{\Theta}_t$:

The distribution of $\boldsymbol{\Theta}_t = (\boldsymbol{\Theta}_{Dt}, \boldsymbol{\Theta}_{Mt})'$ conditional on V_t and on $\mathbf{I}_t$ is given by

$$(\boldsymbol{\Theta}_t | \, V_t, \mathbf{I}_t) \sim N \left[\mathbf{a}_t^*, S_t R_t^* S_t \right]$$

and the distribution of V_t conditional on $\mathbf{I}_t$ is an inverse-Wishart with parameters d_t and Ψ_t,

$$V_t | \mathbf{I}_t \sim IW \left[\Psi_t, d_t \right]$$

where $\mathbf{a}_t^* = \mathbf{a}_t + A_t\mathbf{e}_t$, $R_t^* = S_t(R_t - B_t Q_t B_t')S_t$, $S_t^2 = \Psi_t/d_t$, $d_t = d_{t-1} + 1$

and $\Psi_t = \Psi_{t-1} + S_{t-1}Q_t^{*-1}\mathbf{e}_t\mathbf{e}_t'Q_t^{*-1}S_{t-1}$

with $Q_t = Q_t^{*2}$, $B_t = R_t Q_t^{-1}$ and $A_t = S_t B_t S_t^{-1}$ and $\mathbf{e}_t = (\mathbf{Y}_{Dt} - H_t\mathbf{m}_{t-1}, \mathbf{Y}_{Mt} - GH_t\mathbf{m}_{t-1})'$, being the one-step-ahead forecasting error vector.

B.5 The k-steps predictive distribution for $\mathbf{Y}_{t+k}$:

The k-steps ahead predictive distribution for $\mathbf{Y}_{t+k}$ given $\mathbf{I}_t$ is a multivariate Student-t distribution with mean $\mathbf{f}_t(k)$ and covariance matrix $S_{t-1}(k)Q_t(k)S_{t-1}(k)$ where $k = 1, 2, ...$ That is,

$$(\mathbf{Y}_{t+k}|\mathbf{I}_t) \sim T\left[\mathbf{f}_t(k), S_{t-1}(k)Q_t(k)S_{t-1}(k), d_{t-1}(k)\right]$$

where $\mathbf{f}_t(k) = \mathbf{a}_t(k)$ and $Q_t(k) = R_t(k) + I$,
with $\mathbf{a}_t(k) = H_{t+k}\mathbf{a}_t(k-1)$ and $R_t(k) = H_{t+k}R_t(k-1)H_{t+k}' + W_{t+k}$,
where $\mathbf{a}_t(0) = \mathbf{a}_t^*$ and $R_t(0) = R_t^*$,
and $S_{t-1}(0) = S_{t-1}$ and $d_{t-1}(0) = d_{t-1}$,
with $\mathbf{a}_t^*$, R_t^* are defined in B.4,
and S_{t-1} and d_{t-1} are defined in B.3.

References

Anderson, T. W. (1984). *An Introduction to Multivariate Statistical Analysis*. John Wiley & Sons: New York, 2nd edition.

ApSimon, H., Wilson, J., and Simms, K. (1989). Analysis of the dispersal and deposition of radionuclides from chernobyl across europe. *Proc. R. Soc. Lond. A*, **425**, 365–405.

Barbosa, E. and Harrison, J. (1992). Variance estimation for multivariate dynamic linear models. *Journal of Forecasting*, **11**, 621–628.

Bleher, M. and Jacob, P. (1993). Assessment of radionuclide deposition by park. *Radiation Protection Dosimetry*, **50**, 343–348.

Böllmann, U., Eder, E., Starke, H., Stein, H., and Zeising, H. (1987). Auswirkungen des reaktorunfalls in tschernobyl auf bayern. schriftenreihe. Heft **82**. Bayerisches Landesamt fur Umweltschutz.

Castronovo, F. P. (1999). Teratogen update: Radiation and chernobyl. *Teratology*, **60**, 100–106.

Cressie, N. A. C. (1993). *Statistics for Spatial Data*. John Wiley and Sons, NY, revised edition edition.

Gamerman, D., Salazar, E., and Reis, E. (2006). Some applications of dynamic gaussian process priors to the analysis of space-time data models. Valencia. ISBA 8th World Meeting on Bayesian Statistics, Benidorm (Alicante, Spain).

Goldstein, M. (1976). Bayesian analysis of regression problems. *Biometrika*, **63**, 51–58.

Lauritzen, B. and Mikkelsen, T. (1999). A probabilistic dispersion model applied to the long-range transport of radionuclides from the chernobyl accident. *Atmospheric Environment*, **33**, 3271–3279.

Lauritzen, B., Baklanov, A., Mahura, A., Mikkelsen, T., and Sorensen, J. H. (2006). K-model description of probabilistic long-range atmospheric transport in the northern hemisphere. *Atmospheric Environment*, **40**, 4352–4369.

Le, N. D. and Zidek, J. V. (1992). Interpolation with uncertain spatial covariances : A bayesian alternative to kriging. *Journal of Multivariate Analysis*, **43**(2), 351–374.

Masreliez, C. J. (1975). Approximate non-gaussian filtering. *IEEE Trans. Automat. Control*, **20**, 107–110.

Mikkelsen, T., Larsen, S. E., and Thykier-Nielsen, S. (1984). Description of the risø puff diffusion model. *Nuclear Safety*, **67**, 56–65.

Müller, H. and Pröhl, G. (1993). Ecosys-87: A dynamic model for assessing radiological consequences of nuclear accidents. *Health Physics*, **64**, 232–252.

NEA (2002). Nuclear energy agency. Chernobyl: Assessment of radiological and health impacts. (Available from http://www.nea.fr/html/rp/chernobyl/chernobyl.html.).

Sampson, P. D. and Guttorp, P. (1992). Nonparametric estimation on nonstationary spatial covarince structure. *J. Am. Statist. Ass.*, **87**, 108–119.

Schlather, M. (1999). Introduction to positive definite function and to unconditional simulation of random fields. Technical report, Dept. of Mathematics and Statistics, Lancaster University, UK.

Smedley, C., Grindon, E., Dutton, L., and Vleeshhouwer, D. (1996). Source term estimation based on plant status. RODOS(WG5)-TN(**96**)-02.

Smith, J. (1989). Influence diagrams for statistical modelling. *The Annals of Statistics*, **17**(1), 654–672.

tutiempo.net (2008). (http://www.tutiempo.net/en/Weather/Germany/DE.html).

Walker, S. and Muliere, P. (1997). Beta-stacy processes and a generalization of the polya-urn scheme. *The Annals of Statistics*, **25**(4), 1762–1780.

Watari, K., Imai, K., Ohmomo, Y., Muramatsu, Y., Nishimura, Y., Izawa, M., and Baciles, L. R. (1988). Simultaneous adsorption of cs-137 and i-131 from water and milk on metal ferrocyanide-anion exchange resin. *Journal of Nuclear Science and Technology*, **25**(5), 495–499.

West, M. (1982). Aspects of recursive bayesian estimation. *Unpublished PhD thesis, University of Nottingham*.

West, M. and Harrison, P. J. (1997). *Bayesian Forecasting and Dynamic Models*. Springer-Verlag, New York, 2nd edition.

WNA (2008). World nuclear association: Chernobyl accident. (Available from http://www.world-nuclear.org/info/chernobyl/inf07.html.).